VOLUME 5, NUMBER 1

Geotechnical Journal

DECEMBER 2011

Sri Lankan Geotechnical Society

Geotechnical Journal

CONTENT

EDITED BY :

Dr. Asiri Karunawardena

ARTICLES REVIEWED BY :

Prof. M Gunaratne
Prof. M R Madhav
Dr. Rajendra Kumar Bhandari
Dr. Priyantha Jayawickrama
Eng. K S Senanayake

ISSN – 1391 – 6149

Sri Lankan Geotechnical Society
C/o National Building Research Organisation
99/1, Jawatta Road, Colombo 5
Sri Lanka

De Silva L.I.N[1]

Development of High Capacity Torsional Shear Apparatus for the Measurement of Small Strain Deformation Properties of Soils

ABSTRACT: Recently developed medium-sized torsional shear apparatus at Institute of Industrial Science, University of Tokyo, Japan and results from tests on dry Toyoura sand using a modified version of pin-typed local deformation transducer (PLDT) system with other conventional strain measurement techniques are presented.

Loading system of this apparatus consists of servo motors coupled with reduction gear systems for controlling both vertical and torsional loadings precisely. This apparatus is capable of controlling both vertical and torsional cyclic loading either by stress amplitude or strain amplitude. Cell pressure can be controlled by an electro-pneumatic transducer. The three stress components (axial, torsional and confining stress) can be controlled independently by using a personal computer. High loading capacity of the apparatus and its capability of testing specimens of various sizes up to 20 cm in outer diameter, 12 cm in inner diameter and 30 cm in height are helpful in understanding the properties of geomaterials with large particle sizes such as gravel.

Axial and torsional loads are measured precisely with a two-component load cell, which has a negligible coupling effect. Cell pressure is measured by using a high capacity differential pressure transducer. In order to measure the local strains, two sets of PLDT's arranged in a triangular form using separate hinges are used at opposite sides of a diameter of the specimen.

Based on cyclic torsional shear and triaxial tests on dry Toyoura sand using this apparatus, it was confirmed that quasi-elastic deformation properties such as Young's modulus and shear modulus can be measured at various stress states by conducting small amplitude cyclic loading in axial and torsional directions.

In addition, it was verified that this apparatus is capable of conducting large cyclic drained and undrained loadings and hence liquefaction behavior of sand can be investigated.

Introduction

Since the strain level for ground deformation under normal working loads is usually less than 0.5 %, determination of the quasi-elastic deformation properties such as Young's modulus and shear modulus of various soils under different stress levels plays an important role in designing civil engineering structures. However, the system compliance problems in laboratory soil testing apparatuses, such as end restraint effects and bedding errors, lead to less reliable results in externally measured (measured outside the cell) deformation properties of soils. Therefore, local measurement of small strains in soil testing is gaining higher popularity among researchers due to its closeness to the actual deformation. In the triaxial tests on soils, as summarized by Scholey et al. (1995), the recent developments on small strain measurement techniques by static methods, such as inclinometer, proximity transducer, local deformation transducer (LDT, Goto et al., 1991), among others, have made it possible to investigate the behavior of soil at strain levels less than 0.001 %, which is known as quasi-elastic.

[1]**Senior Lecturer, Department of Civil Engineering, University of Moratuwa, Sri Lanka**

On the other hand, use of the local measurement in hollow cylinder specimens is still limited, although hollow cylinder apparatus is an effective tool in studying the behavior of soil including the rotation of principal stress axes. Among other local measurements, Hong Nam (2004) has applied a set of LDTs in a triangle form to hollow cylinder specimens. With this device, by applying small cyclic loading in the course of any stress path, quasi-elastic properties can be measured. However, its full applicability has been verified only on relatively large specimens with dimensions of 20 cm in outer diameter, 12 or 16 cm in inner diameter and 30 cm in height, as described in detail later. In addition, the hollow cylinder apparatus employed by Hong Nam (2004) had a limited loading capacity; the maximum axial and torsional shear stresses that could be applied to the above hollow cylinder specimen having an inner diameter of 12 cm were 400 kPa and 92 kPa, respectively. Therefore, in this study, in order to investigate into the quasi-elastic deformation properties of relatively stiff geomaterials under various stress states, a high-capacity medium-sized hollow cylinder apparatus is newly developed, and the local measurement system that was originally developed by Hong Nam (2004) is modified so that it can be applied to smaller specimens. Preliminary test results on dry dense Toyoura sand by using these devices are presented as well.

High Capacity Medium-sized Hollow Cylinder Apparatus

To meet the above mentioned engineering needs, a hollow cylinder apparatus with a higher loading capacity was newly developed at Institute of Industrial Science, University of Tokyo, Japan. The new apparatus can be characterized by the following features.

1. Fully automated stress or strain path control
2. Application of very small unload-reload cycles at any stress state in both axial and torsional directions independently to evaluate Young's modulus, shear modulus and Poisson's ratio of geomaterials.
3. Accurate local measurement of strains from amplitude less than 0.001 % up to failure.
4. High loading capacity with an internal two-component load cell.

As shown in Fig. 1, the basic components of the system consist of a triaxial cell, axial and torsional loading systems, a pneumatic cell pressure system, local and external transducers and a personal computer equipped with a control and measurement program. The digital signals from the control program are converted into analog signals using two 12-bit D/A converters. Analog electric signals from the transducers are amplified using dynamic strain amplifiers and converted into digital signals using two 16-bit A/D converters. These data are then stored in the computer and transferred to the control program to control the stress path.

The apparatus is capable of testing hollow cylindrical specimens with various sizes up to outer diameter of 20 cm, inner diameter of 12 cm and a height of 30 cm. In this study, specimens having outer diameter of 15 cm, inner diameter of 9 cm and a height of 30 cm were used, since this specimen size is preferable in testing in-situ frozen samples, which are usually available with the size of 15 cm in diameter.

The vertical loading parts are driven by an AC servo motor which is connected to the loading shaft through a series of reduction gears, two sets of electro magnetic clutches, one electro-magnetic brake and a ball screw with a pre-pressurized nut. Refer to Santucci de Magistris et al. (1999) for the detailed performances of this vertical loading system that had been employed for triaxial tests on solid cylindrical specimens. For the present apparatus, another set of similar systems was employed for the torsional loading parts. Axial and torsional loading capacities are 15 kN and 0.3 kN.m, respectively. The maximum axial and torsional shear stresses that could be applied to the largest specimen as described above are 740 kPa and 180 kPa, respectively. This loading device is a displacement controlled type from a mechanical point of view, while cyclic axial and torsional tests by keeping a specified stress amplitude can also be conducted by using a personal computer which monitors the outputs from a two-component loadcell with a negligible coupling effect and controls the loading device accordingly. Cell pressure can be controlled by an electro pneumatic transducer with a capacity of 1000 kPa.

This apparatus is currently equipped with 16 measuring channels. Axial and torsional loads were measured with the high capacity two-component loadcell. Cell pressure was measured by using a high capacity differential pressure transducer (HCDPT). Measurement of volume change inside the specimen can be made with an electronic balance with an accuracy of 0.001g. Two external displacement transducers (LVDTs) were employed for external measurement of axial strain and the output from them were used for controlling axial loading by strain amplitude. One potentiometer attached to the top cap was used for the measurement of the rotation of the specimen and the output was used to control the torsional loading by strain amplitude. In addition, three proximity transducers also known as Gap Sensors (GS1, GS2 and GS3 as of Fig. 4), ranged 4 mm, were used for the external measurement of axial and shear strains.

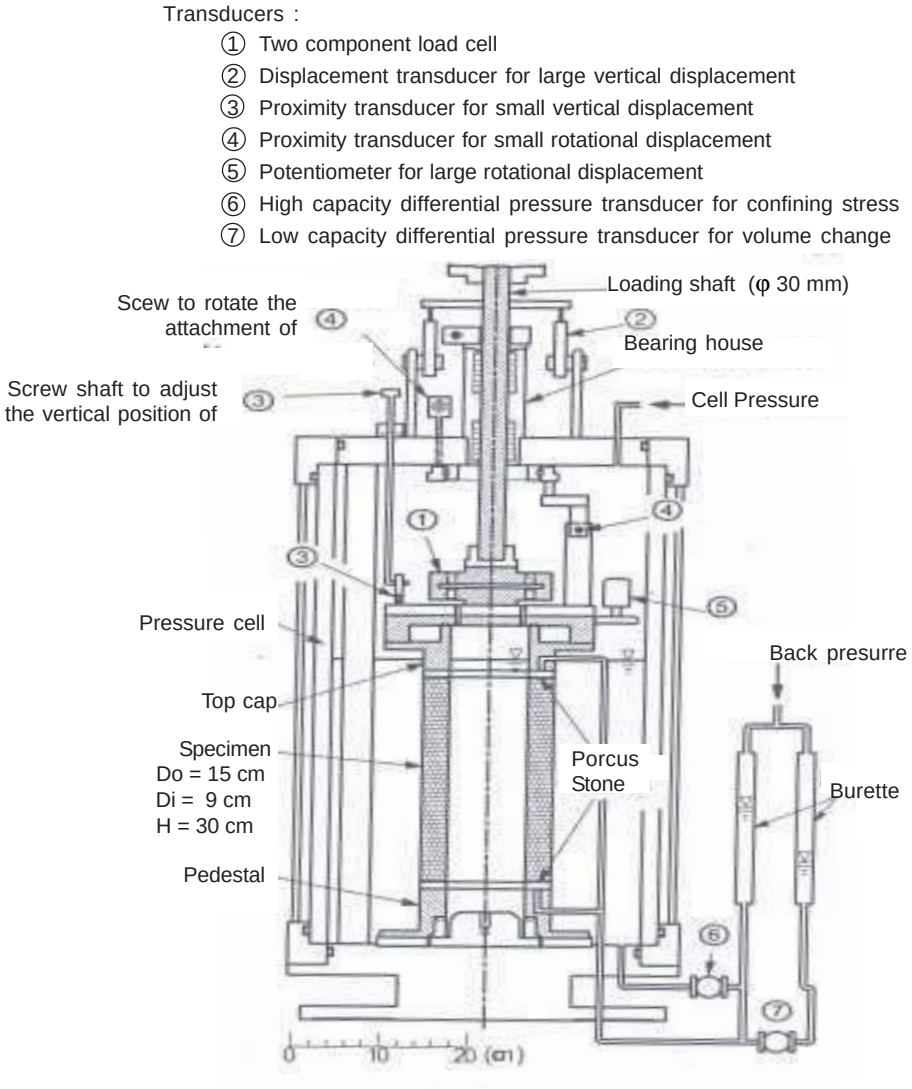

FIG. 1. Triaxial cell and transducers

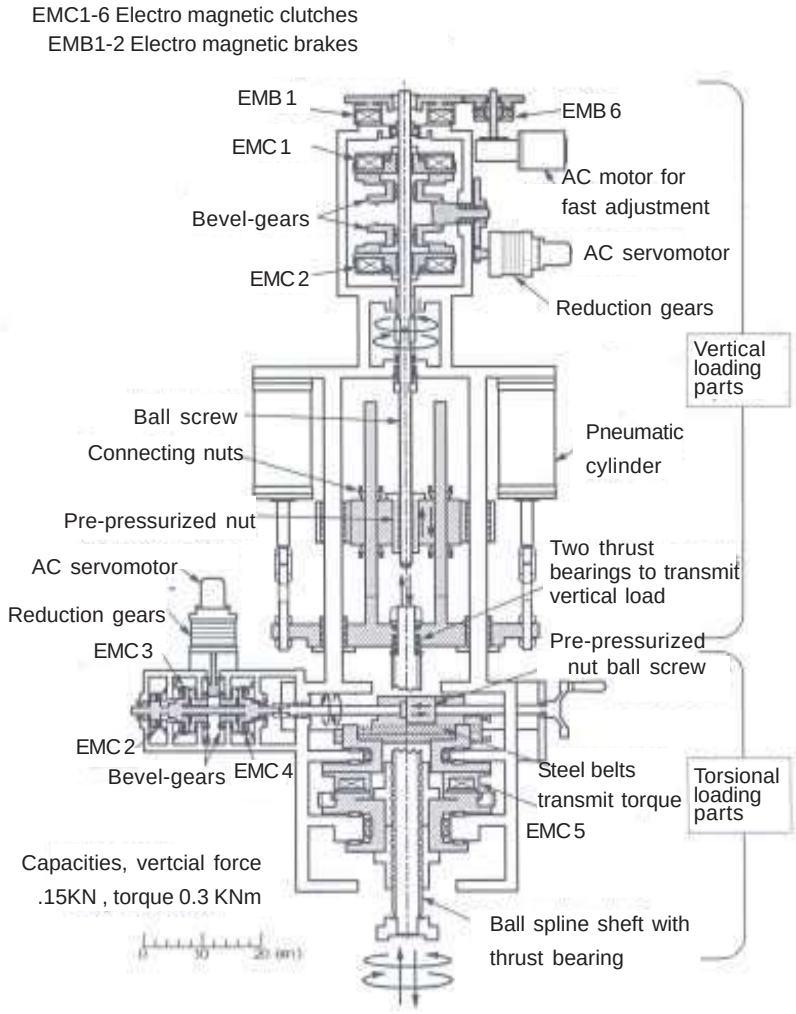

FIG. 2. Axial and torsional loading system

Local Strain Measurement

The basic principle behind the local strain measurement technique employed for this study is simple. The original concept (Hong Nam et al., 2001; Hong Nam, 2004, Hong Nam et al., 2005) employed three local deformation transducers with pinned ends, called pin-typed local deformation transducer (PLDT), arranged in a shape of a triangle using special hinges glued directly to the specimen. This hinge has a conical hole to support the pinned end of the PLDT. The original version of PLDT employed one hinge to support two PLDTs. In principle, a vertical PLDT measures axial deformation; a horizontal PLDT measures the changes in outer diameter; and a diagonal PLDT measures the shear strain. However, as typically shown in Fig. 3a, it was found that this original system does not work properly, as compared to the external measurements for specimens with outer diameter 15 cm (Fig. 3b).

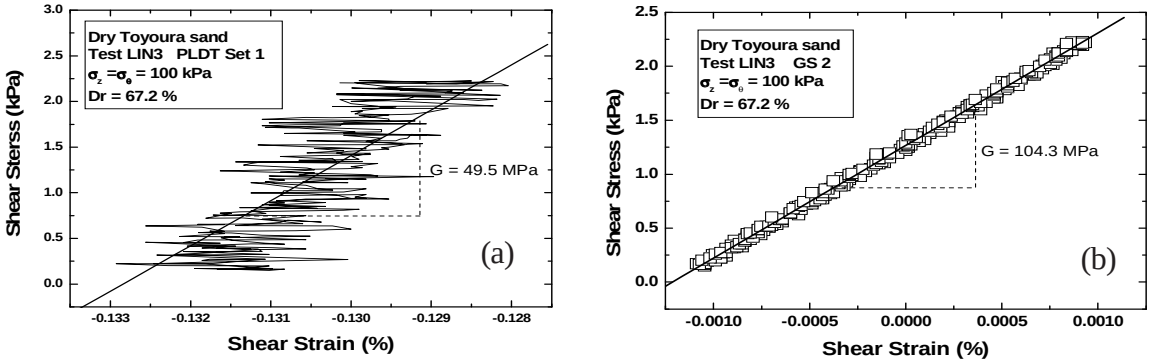

FIG. 3. Evaluation of G using (a) original version of PLDT; and (b) external transducer

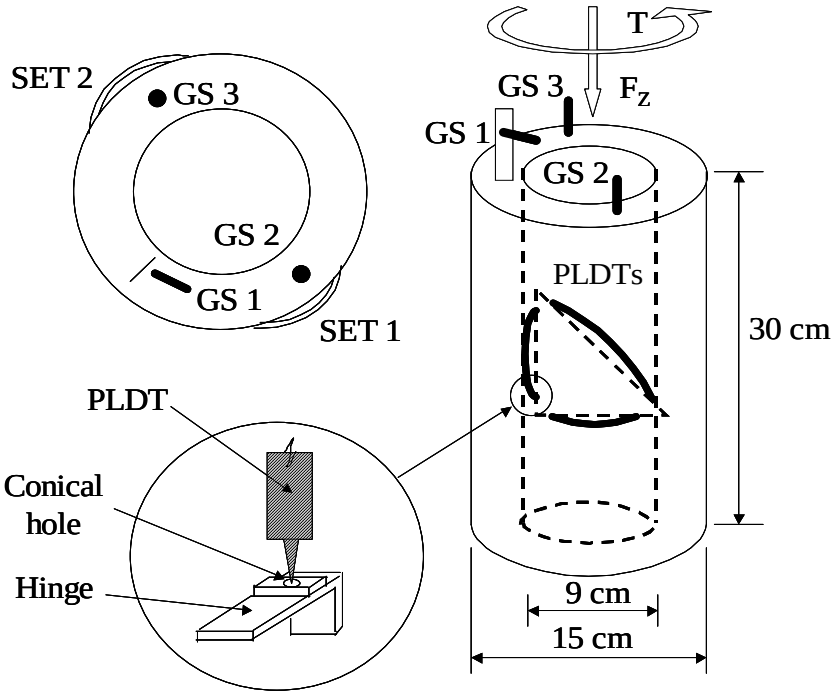

FIG. 4. Arrangement of PLDTs and proximity transducers (GS1, GS2 and GS3)

Therefore the original version was modified by supporting the three PLDTs with six separate hinges. Fig. 4 illustrates the layout of the modified version of PLDT and other transducers used in this study.

Two sets of the modified version of PLDTs (SET1 and SET2) arranged symmetrically along a diameter of specimen at the middle height were used for local strain measurement. Free lengths of PLDTs were 10.2 cm, 5.5 cm and 8.1 cm for the vertical, horizontal and diagonal ones, respectively. An attempt was made to set the diagonal PLDT at an angle of 45^0 to the horizontal to optimize the shear strain measurement. No PLDT was placed along the inner surface of the specimen due to limited working space.

Calculation of local strains using modified version of PLDTs

The basic concept of strain calculation employed for the PLDT system is based on two main assumptions that the central angle (θ_0) subtended by the horizontal PLDT (XY in Fig. 5) remains constant during loading and that the specimen keeps its right hollow cylindrical shape.

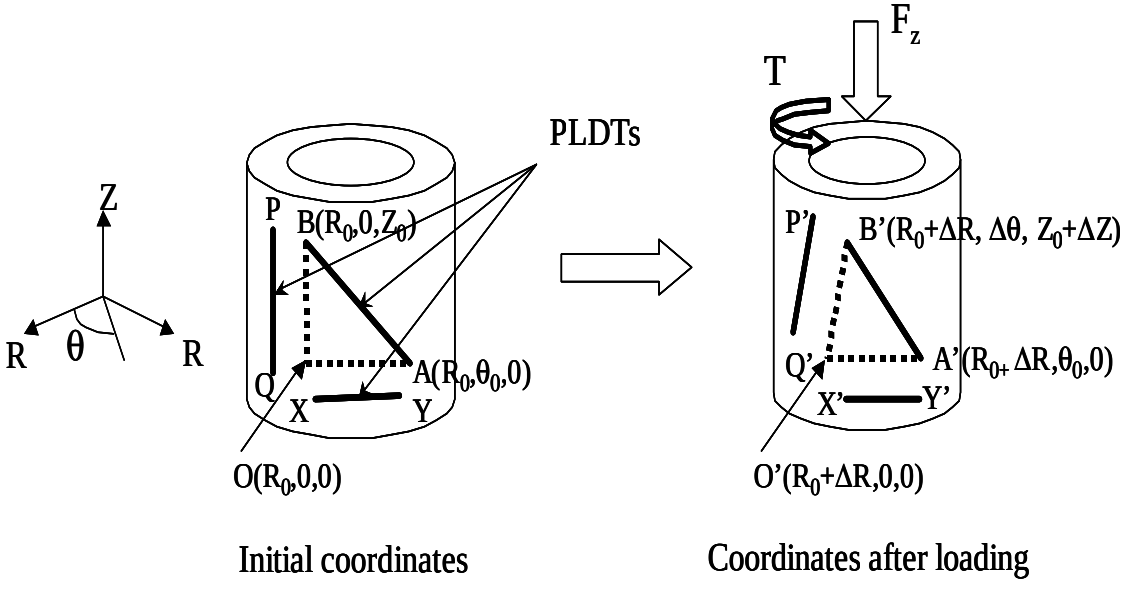

FIG. 5. Basic concept of strain formulation in modified version of PLDTs

This system has three unknowns (ΔR, Δθ, ΔZ) for the change in coordinates to be determined from three equations (lengths X'Y', A'B' and P'Q' of each PLDT). For the modified version of PLDT system, as shown in Fig. 5, the strains in O'B' and O'A' after loading are assumed to be the same as those in P'Q' and X'Y', respectively. Thus the three unknowns can be formulated as follows.

$$\Delta R_o = R_o \left(\overline{O'A'} / \overline{OA} - 1 \right) \quad \text{.....(1)}$$

$$\Delta\theta = \theta_o/2 - \arcsin\{[\overline{A'B'}^2 - \overline{O'B'}^2] / [4R_o^2 \sin(\theta_o/2)]\} \quad \text{..(2)}$$

$$\Delta Z = [\overline{O'B'}^2 - 2R_o^2 (1 - \cos\Delta\theta)]^{0.5} - Z_o \quad \text{.....(3)}$$

Using the above equations, it is possible to evaluate ε_θ, ε_z, and $\gamma_{z\theta}$ locally.

Typical test results

The material used for this study was air-dried Toyoura sand (D_{50} = 0.162 mm, uniformity coefficient = 1.46, e_{min} = 0.600 and e_{max} = 0.966), a widely tested Japanese sand. As mentioned before, test specimens have dimensions of 15 cm in outer diameter, 9 cm in inner diameter and 30 cm in height. All the specimens were prepared by air pluviation, while varying the falling height of sand particles from 30 cm to 1 m. Relative densities of the specimens are in the range of 72.8 % to 90.6 %. All the tests were conducted under drained condition. First, all the specimens were isotropically consolidated (IC) from $\sigma'_z = \sigma'_\theta = \sigma'_r$ = 30 kPa to 400 kPa and unloaded to 50 kPa (refer to Fig. 5 for definition of coordinate system). Then the specimens were triaxially sheared (TC) up to σ'_z = 250 kPa while keeping $\sigma'_\theta = \sigma'_r$ at 50 kPa. Eleven unload-reload cycles in both vertical and torsional directions with single strain amplitude of about 0.001 % and 0.0015 %, respectively, were applied after each 50 kPa increment of vertical stress in IC and 25 kPa increment in TC. The 10th cycle in each cyclic loading was used to evaluate small-strain Young's and shear moduli. Fig. 6 shows typical records of eleven small unload reload cycles in both axial and torsional directions with time.

Typical evaluation of the vertical Young's modulus E and the shear modulus G on vertical and horizontal planes using the modified version of PLDT is shown in Fig. 7.

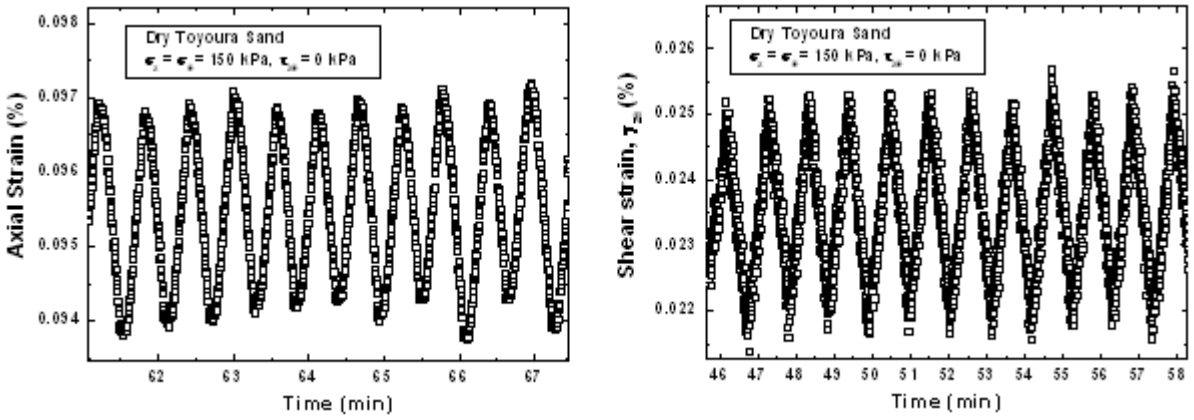

FIG. 6. Axial and shear strains vs. time measured by modified version of PLDTs

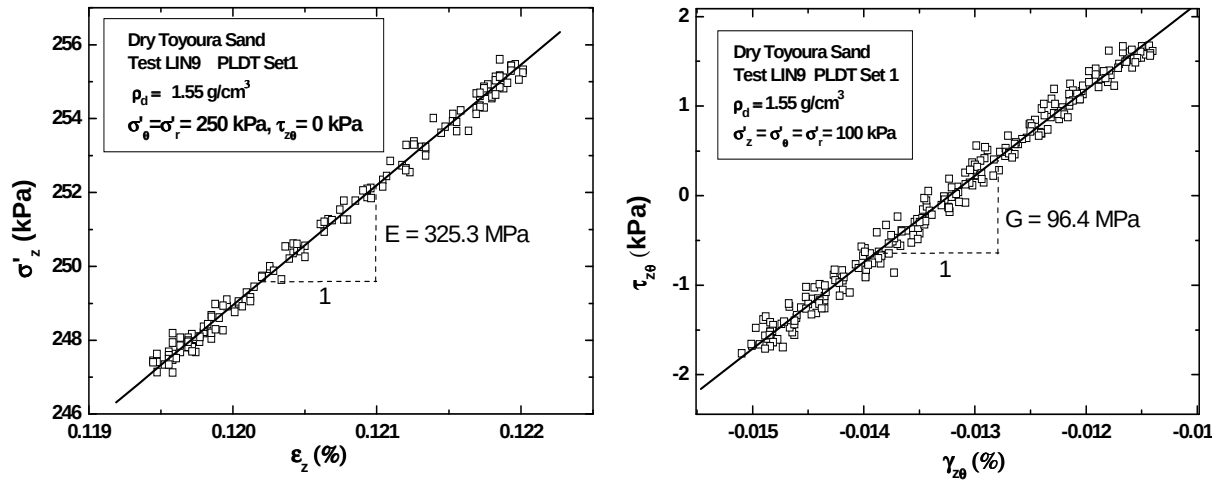

FIG. 7. Typical evaluation of E and G using the modified version of PLDT

Comparison of externally and locally measured E and G are shown in Fig. 8. E is evaluated from the output of four transducers namely, two proximity transducers (GS2 and GS3) and two sets of PLDTs. It can be seen that the results from all the transducers are similar to each other with an average difference of about 2 %. On the other hand, G values evaluated using external transducers namely, potentiometer (POT2) and GS1 are on average 15 % greater than the locally measured ones by two sets of PLDTs. However, the results using different transducers are consistent with each other in terms of their stress state dependencies (i.e., the m and n values, as defined in Fig. 8 are similar irrespective of the measurement devices). This verifies the results from previous studies (Hong Nam and Koseki., 2003, 2005; Hong Nam et al., 2005) on the same material using the original version of PLDTs.

Fig. 9 explains a possible reason for the difference in externally and locally measured shear modulus inferred by assuming no slippage between the top cap, pedestal and the specimen. The friction blades of the top cap and pedestal restrain the free movement of top and bottom layers of soils, which have a thickness at least equal to the height of the blades. This is creating a non-uniform distribution of shear strains along the specimen height, as shown in the figure. Therefore shear strain (γ) measured externally is smaller than that measured locally, which yields higher shear modulus from external measurements than that from local measurements. Theoretically, the difference between external and local measurements should reduce with the increase of the specimen height.

Values of E and G for specimens with different densities measured during isotropic consolidation (IC) using the modified version of PLDTs are shown in Fig. 10. After normalizing by the void ratio function f(e), as proposed originally by Hardin and Richart (1963) and shown in the figure, all the specimens showed rather a unique relationship against stress levels. These relationships were almost the same as those shown in Fig. 11, which has been obtained by Hong Nam and Koseki (2005) using the original version of PLDTs on larger specimens with 20 cm in outer diameter, 12 cm in inner diameter and 30 cm in height.

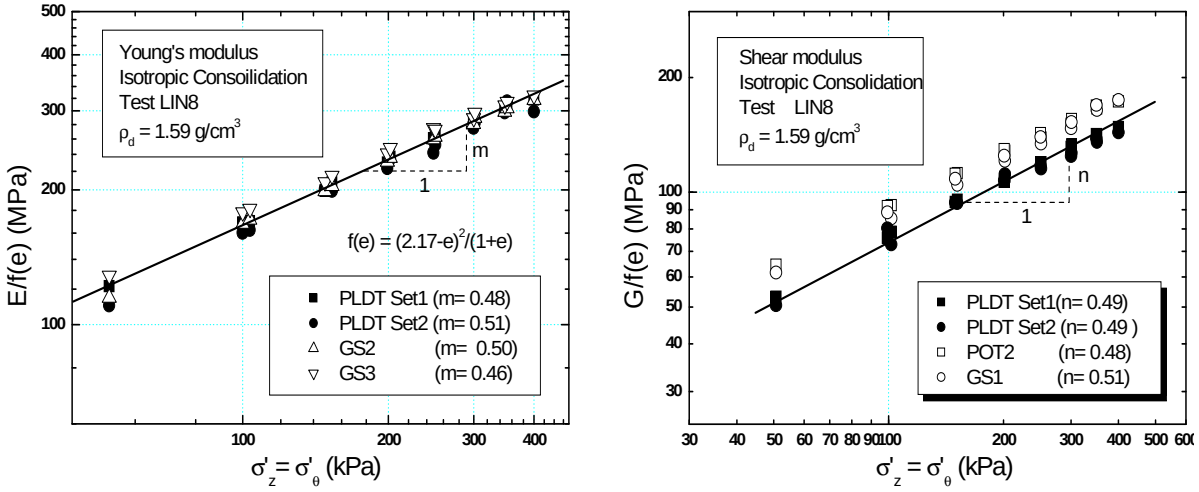

FIG. 8. Comparison of externally and locally measured E and G

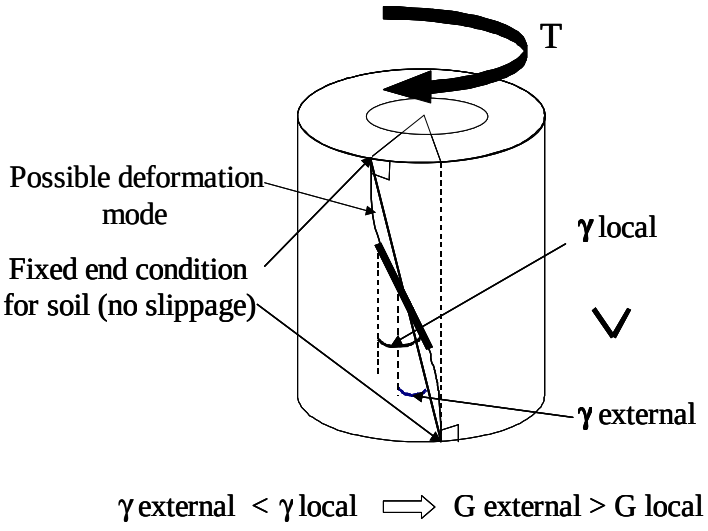

FIG. 9. Possible reason for the difference in externally and locally measured G

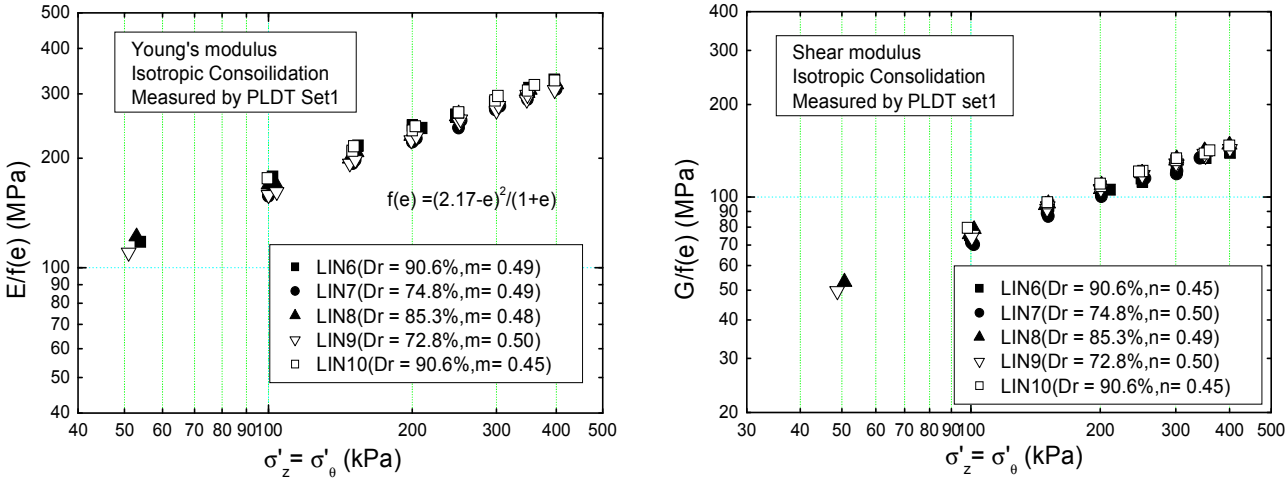

FIG. 10. Comparison of E and G at various densities using modified version of PLDTs

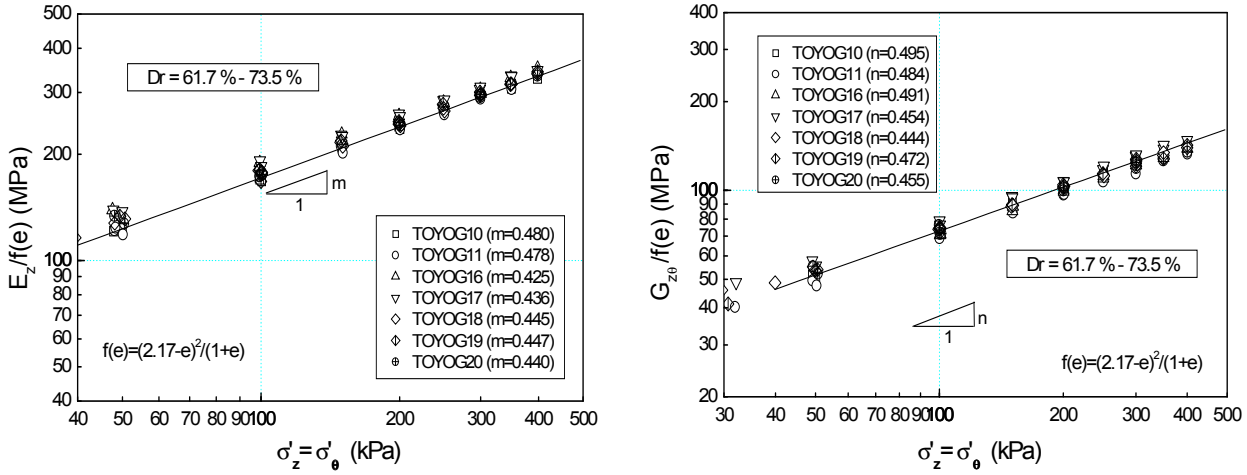

FIG. 11. E and G using the original version of PLDTs on larger specimens (after Hong Nam and Koseki 2005)

Fig. 12 illustrates the effect of principal stress ratio on locally measured Young's and shear moduli during triaxial compression. The Young's modulus showed a continuously increasing trend, while the shear modulus showed a sudden degradation after the principal stress ratio $R = \sigma'_z/\sigma'_\theta$ exceeded three. The latter trend is consistent with the results from the previous studies by Yu and Richart (1984), Chaudhary et al (2004) and Hong Nam (2004). The degradation in shear modulus is due possibly to the damage to the soil structure at high shear stress states. Note that the Young's modulus values of test LIN10 are greater than those of the other tests because the specimen for test LIN10 was sheared at a higher confining pressure (σ_θ =150 kPa).

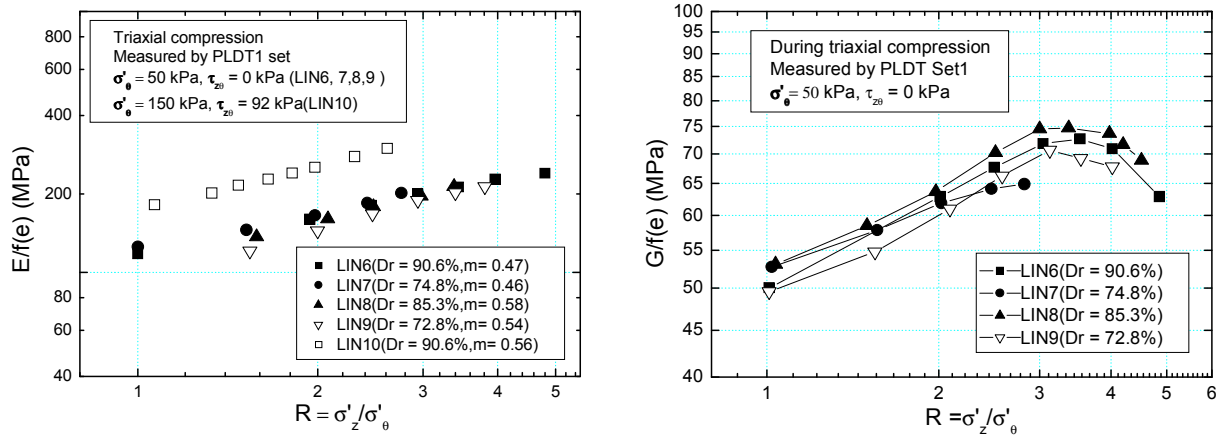

FIG. 12. Effects of principal stress ratio on Young's and shear moduli

Conclusions

It was confirmed that the recently developed high capacity medium sized hollow cylinder apparatus can be effectively used for controlling and measuring strains less than 0.001 % in both axial and torsional directions. In addition, the modified version of PLDT system can be successfully used to measure quasi-elastic deformation properties of geomaterials. Locally and externally measured Young's and shear modulus values are consistent with each other in terms of their stress state dependencies. The locally measured shear moduli were by about 15 % larger than the externally measured ones, while Young's moduli showed insignificant difference between local and external measurements. This behaviour may be due to the possible non-uniform distribution of shear strains along the specimen height. When normalized by the void ratio function, locally measured Young's and shear moduli for specimens with various densities showed a unique relationship against stress levels. A sudden degradation of locally measured shear modulus at the principal stress ratios greater than three was observed.

References

Chaudhary, S. K., Kuwano, J. and Hayano, Y. (2004). "Measurement of quasi-elastic stiffness parameters of dense Toyoura sand in hollow cylinder apparatus and triaxial apparatus with bender elements." *Geotechnical Testing Journal*, ASTM, 27 (1), 23-35.

Goto, S., Tatsuoka, F., Shibuya, S., Kim, Y.S. and Sato, T. (1991). "A Simple Gauge for Local Small Strain Measurement in the Laboratory." *Soils and Foundations*, 31(1), 169-180.

Hardin, B. O. and Richart, F.E. (1963). "Elastic Wave Velocities of Granular Soils." *Journal of Soil Mechanics and Foundation*, ASCE, 89(1), 33-65.

Hong Nam, N., Sato, T. and Koseki, J. (2001). "Development of Triangular Pin-typed LDTs for Hollow Cylindrical Specimen." *Proceedings of 36th annual meeting of JGS*, 441-442.

Hong Nam, N. and Koseki, J. (2003). "Quasi-elastic Shear Modulus of Toyoura Sand with Local Strain Measurement." *Proc. of the Fifth International Summer Symposium*, JSCE, Tokyo, 237-240.

Hong Nam, N. (2004). "Locally Measured Deformation Properties of Toyoura Sand in Cyclic Triaxial and Torsional Loadings and Their Modelling." *PhD. Thesis*, The University of Tokyo.

Hong Nam, N. and Koseki, J. (2005). "Quasi-elastic Deformation Properties of Toyoura Sand in Cyclic Triaxial and Torsional Loadings." *Soils and Foundations*, 45(5), 19-38.

Hong Nam, N., Koseki, J. and Sato, T. (2005). "Effect of Specimen Size on Quasi-elastic Properties of Toyoura Sand in Hollow Cylinder Triaxial and Torsional Shear Tests." (Submitted for possible publication in *Geotechnical Testing Journal*, ASTM).

Santucci de Magistris, F., Koseki, J., Amaya, M., Hamaya, S., Sato, T., and Tatsuoka, F. (1999). "A Triaxial Testing System to Evaluate Stress-Strain Behaviour of Soils for Wide Range of Strain and Strain Rate." *Geotechnical Testing Journal*, ASTM, 22(1), 44-60.

Scholey, G. K., Frost, J. D., Lo Presti, D. C. F. and Jamiolkowski, J. (1995). "A Review of Instrumentation for Measuring Small Strains during Triaxial Testing of Soil Specimen." *Geotechnical Testing Journal*, ASTM, 18(2), 137-156.

Yu, P. and Richart, F.E., Jr. (1984). "Stress Ratio Effects on Shear Modulus of Dry Sands." *Journal of Geotechnical Engineering*, ASCE, 110(3), 331-345.

Sujeevan V[1] and Kulathilaka S.A.S[2]

Rainfall Infiltration Analysis in Unsaturated Residual Soil Slopes

ABSTRACT: Rainfall-induced slope failure is a common geotechnical problem in the tropics where residual soils are abundant. Residual soils are formed due to the weathering of rocks and lie at the location of the parent rock. They are characterized by the significant variations in the level of weathering and the composition of the weathered product over short distances. Quite often, the ground water table is low during the dry season and these soils are in an unsaturated state.

The shear strength of the unsaturated soils is enhanced due to presence of matric suction. With the infiltration of rainwater, the matric suction will be depleted for some depth. As the rain progresses the depth of depletion increases. This aspect was studied in this research with an infiltration model. The model was applied initially to a slope formed of homogeneous soil and later to a slope where two layers of significantly different levels of weathering exist.

In this study, simulated rainfalls of different intensities and durations representative of tropical climatic conditions were applied to the two different cut slope of southern highway in Sri Lanka. Each Cut slope was analyzed by having different types of weathering profiles.

A finite element computer package SEEP/W2007 was used to simulate the infiltration through unsaturated soil.

Key Words

Matric suction; Rainfall; Unsaturated soil; Infiltration

Background

Rain induced slope failures are a major challenge encountered by Sri Lankan geotechnical engineers. Most slopes in Sri Lanka are formed by residual soils. The weathering process involved in the formation of residual soils results in significant variation within the soil due to mineralogical composition of the parent rock which is metamorphic. The degree of weathering and the mineralogical composition of the weathered product can vary in an abrupt manner. The presence of relict discontinuities adds further complexity to the problem.

These slopes are generally with a low ground water table during the dry season and prevailing matric suctions enhances the stability of the slope. Infiltration of rainwater into these slopes is affected by factors such as; the complex geological condition, nature of the soil and rock material present, antecedent soil moisture content etc. In this study, the complex natural condition was idealized with a simpler model and the effect of prolonged rainfall on the pore pressure regime was studied for different rainfall intensities.

Methodology

The analysis was performed on two typical cut slopes in the southern expressway project. Cut slopes were of different gradients. Considering the highly variable conditions encountered, three different sub soil conditions were studied in the project. The Case 1 was a slope made of a uniform residual soil. In Case 2, a less weathered layer(Weathered Rock-WR) underlies a thick residual soil layer. In Case 3, the less weathered layer underlies a thin residual soil layer. The second layer (WR) is with greater shear strength and lower permeability. This is a situation seen in many typical slopes in the country.

Infiltration of the rainwater through the unsaturated soil slope and the resulting changes in the pore pressure regime was analyzed by the SEEPW-2007 computer package

Saturated and Unsaturated Soils

All the voids in a soil below the ground water table are filled with water and the soil is in a saturated state. Above the ground water table some voids are filled with air and the soil is in an unsaturated state and a three phase system exists with solids, water and air. Consequently, both pore water pressure (u_w) and pore air pressure (u_a) should be considered in an analysis. The pore air pressure is usually equal to the atmospheric. The pore water pressure above ground water table is less than atmospheric and the variation is presented in a simplified form as full line in Figure 1. Providing a limit to the practically possible maximum matric suction, a more realistic distribution is presented in broken lines in Figure1. Two stress variables $\sigma - u_a$ termed net normal stress and (u_a-u_w) termed matric suction are used in the analysis.

In this research both matric suction profiles i.e. one with negative hydrostatic gradient and the other with an upper limit for the matric suction, were considered separately for the analysis.

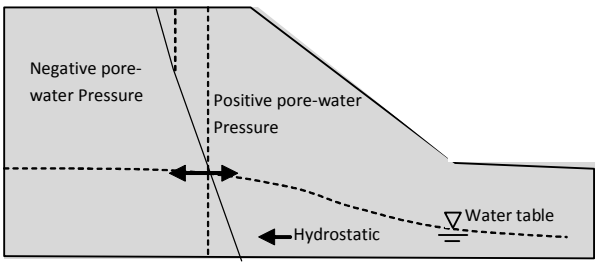

Figure 1: Pore water pressure distribution

Hydraulic Properties of Unsaturated Soil

Similar to the flow through a saturated soil, water flow through an unsaturated soil is generally governed by Darcy's law *(Fredlund and Rahardjo - 1993)*. However, comparing the water flow in an unsaturated soil with the saturated flow, two major differences stand out:

(1) There exits a storage term which represents the variation of water content with matric suction; and

(2) The water coefficient of permeability depends strongly on matric suction.

It should be noted that no volume change in soil is considered during the infiltration process. The storage term in unsaturated

[1]Ph.D Student, University of Southampton, England
[2]Professor, Department of Civil Engineering, University of Moratuwa, Sri Lanka

flow is not a constant but dependent on the suction (or water content) in an unsaturated soil, and can be characterized by the Soil Water Characteristic curves (SWCC). Therefore, SWCC and water coefficient of permeability are the most important hydraulic properties for unsaturated soils.

Soil Water Characteristic Curves (SWCC)

SWCC which shows the variation of the matric suction with the volumetric water content is the most fundamentally important feature in an unsaturated soil.

The volumetric water content is denoted by θ and is defined as;

$$\theta = \frac{V_w}{V_s}$$

V_w- Volume of water content
V_s- Volume of soil

Figure 2 shows an idealized SWCC with two characteristic points A* and B*.Point A* corresponds to the air-entry value *($(u_a$-$u_w)_b$)*, and B* corresponds to the residual water content *(qr)*. As shown in Figure 2, prior to A*, the soil is saturated or nearly saturated, so it can be treated as a saturated. Beyond B*, there is little water in the soil, so the effects of water content or negative pore-water pressure on soil behavior may be negligible.

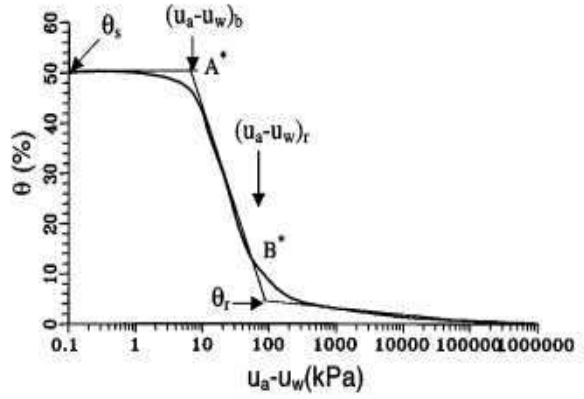

Figure2: Idealized Soil-Water Characteristic Curve

What is of great concern in an unsaturated soils is the stage between A* and B*, in which both air and water phases are continuous or partially continuous, and hence the soil properties are strongly related to its water content or negative pore-water pressure.

Hydraulic Conductivity Function

For an unsaturated soil, the water coefficient of permeability depends on the degree of saturation or negative pore-water pressure of the soil. Water flows only through the pore space filled with water (air-filled pores are not conductive to water), so the percentage of the voids filled with water (i.e., degree of saturation) is an important factor.

The relationship of the degree of saturation to negative pore-water pressure can be represented by a SWCC. Therefore the water coefficient of permeability for unsaturated soils with respect to negative pore-water pressure bears a relationship to the SWCC, and it can be estimated from the saturated permeability and the SWCC *(Fredlund et al. 1994)*.

Hence, a water permeability function of unsaturated soils can be approximated in terms of saturated permeability, air-entry value, de-saturation rate, saturated and residual volumetric water contents.

In consideration of flow through an unsaturated soil, the major difference from the saturated case is the existence of a storage term. This storage term is not a constant but depends on the matric suction. There will be no overall volume change during the infiltration process.

Theory of infiltration through unsaturated soil

According to the Darcy-Buckingham equation, horizontal and vertical water flux (q_x and q_z) in unsaturated soil are expressed as follows:

$$q_x = -k(\psi)\left(\frac{\partial \psi}{\partial x}\right) \qquad \text{-01}$$

$$q_z = -k(\psi)\left(\frac{\partial \psi}{\partial z} + 1\right) \qquad \text{-02}$$

Where k(Ψ) is the hydraulic conductivity as a function of negative pore water pressure Ψ (Martric suction). The equation for continuity of water is expressed as

$$\frac{\partial \theta}{\partial t} = -\left(\frac{\partial q_x}{\partial x} + \frac{\partial q_z}{\partial z}\right) \qquad \text{-03}$$

Where, t is time, Substituting *Equation -01* and *Equation -02* into *Equation -03* yields the two-dimensional, vertical and horizontal flow equation for soil water (*Richard's Equation*):

$$\frac{\partial}{\partial z}\left(K(\psi)\frac{\partial \psi}{\partial z}\right) + \frac{\partial}{\partial x}\left(K(\psi)\frac{\partial \psi}{\partial x}\right) + \frac{\partial}{\partial z}(K(\psi)) = c(\psi)\frac{\partial \psi}{\partial t} \qquad \text{-04}$$

Where c(Ψ) = $\partial\theta/\partial\psi$ is the water capacity function defined as the slope of the soil water retention curve. Solving *Equation-04* requires the use of models for soil water retention and hydraulic conductivity. *(Mukhlisin and Raihan-2008)*

SEEP/W 2007 solves the Equation-04 directly by using the finite element method. *(GEO-SLOPE International Ltd. -2007)*

Infiltration modeling using SEEP/W-2007

As mentioned earlier cut slopes of two different gradients 1:1 and 1:1.267 with 2m wide berms at vertical intervals of 7.5 were used in the study. The geometry of 1:1 gradient cut slope and the boundary conditions utilized for the transient seepage analysis are shown in Figure 3. In the homogeneous soil (Case 1) the entire slope is made of residual soils and in Case 2 a thick layer of residual soil is underlain by weathered rock. The boundary between the residual soil and the weathered rock is shown by

line IC in Figure 3. Finally in the Case 3 the thickness of the residual soil is much lower and the boundary between the residual soil and the weathered rock is shown by line JC in Figure 3.

A boundary flux, *q*, equal to the desired rainfall intensity, *Ir*, was applied to the surface of the slope. The nodal flux, *Q*, was taken to be zero at the sides of the slope above the water table and at the bottom of the slope to simulate a no flow zone (Figure 3). Equal total heads, *ht*, were applied at the sides of the slope below the water table *(Rahardjo et.al-2007)*. The broken line indicates the initial water table of the slopes and it was taken to be the same for all three cases.

The slope geometry with the gradient of 1:1.267 is shown in Figure 4. Boundary conditions are the same as mentioned for the Figure 3

Analysis was carried out for rainfall intensities of 5mm/hr, 20mm/hr, and 40mm/hr. For each rain fall intensity pore water pressure variation were obtained for; 1, 2, 3, 4 and 5 days after infiltration of rain water.

As the soil hydraulic properties, the accepted parameters normally appropriate for the residual soils were taken from the available literature *(Sun et.al-1998)*. The saturated hydraulic conductivities of the soils are $1x10^{-5}$m/s for residual soils and $1x10^{-7}$m/s for highly weathered rock. The saturated volumetric water contents are taken as 0.45, 0.40 respectively.

The SWCC and hydraulic conductivity function for the residual soils and the weathered rock are given in the Figure 5 and Figure 6 respectively.

The pore water distributions were evaluated for the sections 1-1, 2-2, and 3-3 as shown in Figures 3 and Figure 4. They are at the distances of 25m, 55m, and 70m from the left end.

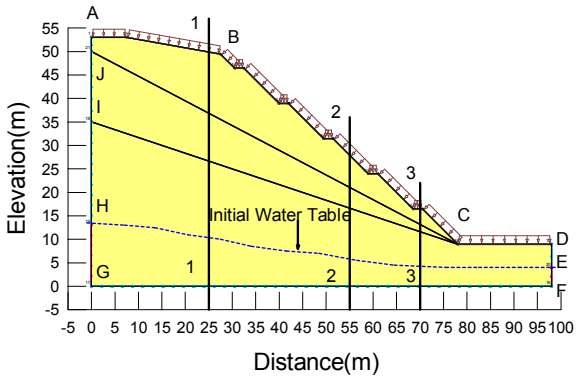

Boundary Conditions

AB, BC, CD= Ir (Rainfall intensity)

AH, DE, FG=Q=0m³/s (No flow Boundary)

EF, GH=ht (Total head at sides)

Figure 3: Cut Slope (1:1) Geometry, Selected Sections and Boundary Conditions

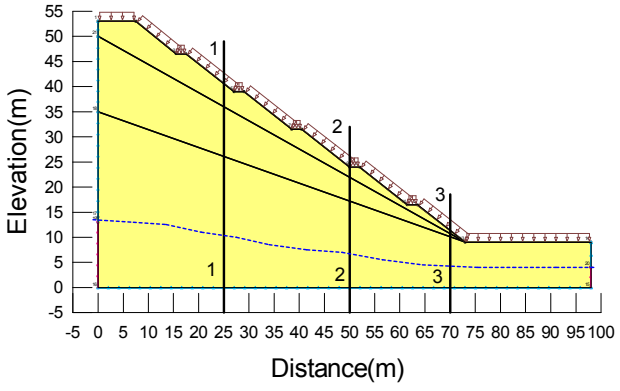

Figure 4: Cut Slope (1:1.267) Geometry, and Selected Sections

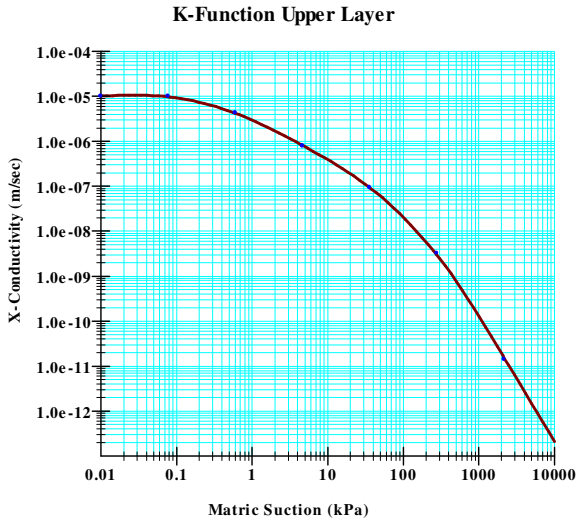

(a) Hydraulic conductivity function

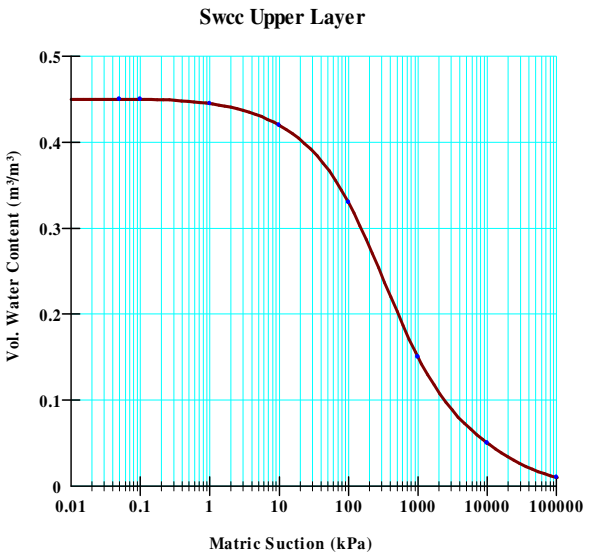

(b) Soil water characteristic curve

Figure 5: Hydraulic Properties of Residual Soil

Initial Pore Water Pressure Matric Suction Profile

Two different initial pore water pressure – matric suction profiles were used in this study. In both profiles pore water pressure was assumed to be hydrostatic below the ground water table. In profile 1, the matric suction in the unsaturated zone was assumed to follow an extension of the same gradient into the negative as shown in full line in Figure 1. In the profile 2, an upper limit was taken for the matric suction as illustrated in broken lines in the same figure.

Effect of Rainwater Infiltration

(a) Initial pwp-matric suction profile 1

The depletion of matric suction and development of positive pore water pressure at the each selected section is presented in Figure 7 for the case of the slope made of uniform residual soil, for a rainfall of intensity 5mm/hr. It could be seen that as the rainfall progressed the depth over which matric suction is lost is increased. This could be termed as progression of the wetting front. The matric suction was lost over a greater depth in section 2-2 and section 3-3 which are towards the lower side of the slope. The upward movement of the ground water table with the progression of rainfall is quite evident in section 2-2 and section 3-3 (Figures 7(b) and 7(c)). For a rainfall of greater intensity - 20mm/hr, the wetting front at the surface progresses to a greater depth. The rise of the ground water table is also more prominent (Figures 8 (a), 8(b) and 8(c)). When the rainfall intensity was increased to 40 mm/hr, the progression of the wetting front and rise of the ground water table were very similar to that of 20mm/hr rainfall. This can be attributed to the fact that the infiltration is controlled by the hydraulic conductivity of the soil. The excess rainfall will contribute to the runoff.

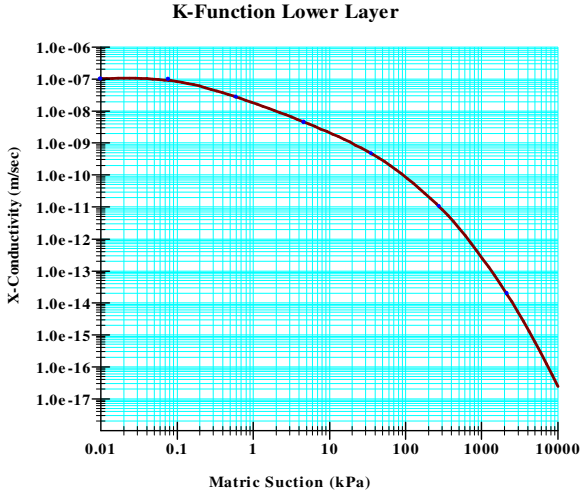

(a) Hydraulic conductivity function

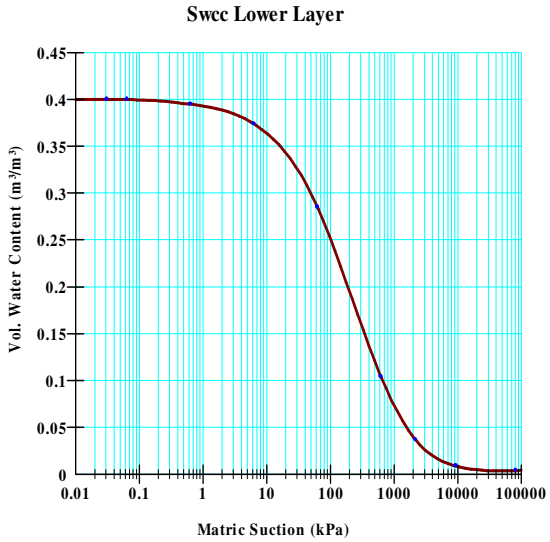

(b) Soil water characteristic curve

Figure 6: Hydraulic Properties of Highly Weathered Rock

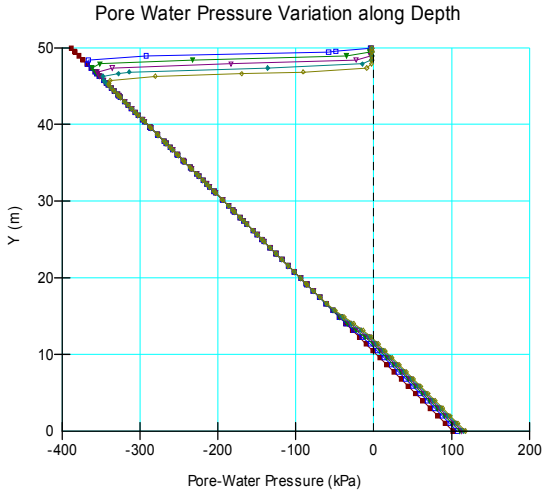

(a) Section 1-1

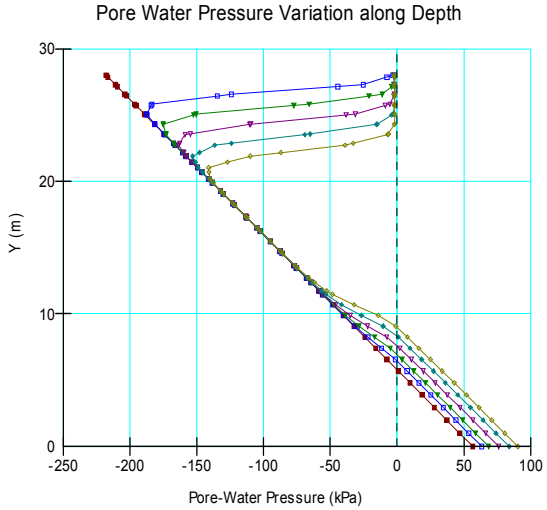

(b) Section 2-2

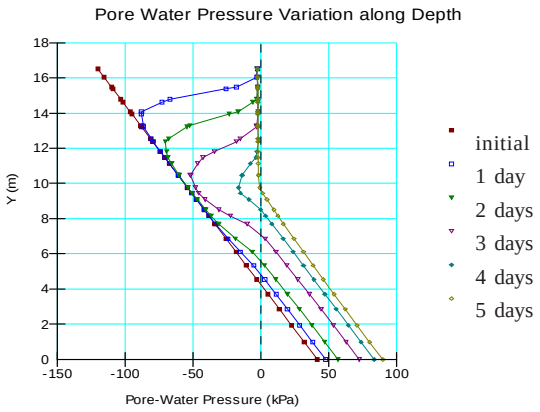

(c) Section 3-3

Figure 7: Results of 5mm/hr Rainfall for Case 1

Weathering profiles are quite variable in Sri Lankan residual soil slopes that are mainly the weathered product of metamorphic rocks. The variations are quite rapid and complex. Nevertheless the degree of weathering is high much closer to the ground surface in general. As such, the complex weathering profiles were simplified in Figure 3 and Figure 4 with a layer of residual soil overlying a layer of weathered rock. Two cases –one with a thick layer of residual soil (Case 2) and another with a much thinner layer of residual soil (Case 3) were considered. The residual soil at the top was with a much grater coefficient of saturated permeability.

Infiltration under these situations (Case 2 and Case 3) were modeled with SLOPEW software for rainfall intensities of 5mm/ hr and 20 mm/hr. The results for the 5mm/hr rainfall for Case 2 are presented in Figure 9. The results for the 20mm/hr rainfall for the same case are presented in Figure 10. Comparison of Figure 7 and Figure 9 indicates that rain water has not infiltrated into the weathered rock layer. As a result positive pre water pressures have built up at the boundary between the two layers. Water table has not gone up in weathered rock in Figure 9 (c) although it has in residual soil in Figure 7 (c). With the increase of the rainfall intensity to 20mm/hr positive pore water pressures have developed even at section 2-2 (Figure 10). This effect is more evident when the thickness of the residual soil layer is much smaller, as indicated in Figure11 (c) for Case 3.

b) Matric suction profile with an upper limit

The matric suction above the water table may not necessarily follow a negative gradient similar to hydrostatic. The matric suction closer to the surface could have an upper limit based on the characteristics of the soil. As such, another series of infiltration studies were done imposing an upper limit of 100 kN/m^2 for the matric suction. The analyses for the Case 1 for rainfall intensities of 5mm/hr and 20 mm/hr are presented in Figure 12 and Figure 13. It could be seen that the wetting front has propagated to a greater depth as compared to the corresponding conditions with the previous matric suction profile (Compare Figure 7 and Figure 12). Hence it is quite evident that the antecedent rainfall and the matric suction profile will have a significant influence on the infiltration response.

With the increase of rainfall intensity to 20mm/hr under the conditions of Case 1, the increase of the rise of the ground water table and the development of positive pore water pressures near the surface are illustrated in Figure 13.

For Case 2, where a weathered rock layer is present underneath the residual soil, larger positive pore water pressures were developed near the surface. There was no rise of ground water table in the weathered rock as the infiltration it was hampered by its low permeability. This was clearly illustrated for a rainfall intensity of 5mm/hr in Figure 14. A perched ground water table condition (positive pore water pressures) has developed at the

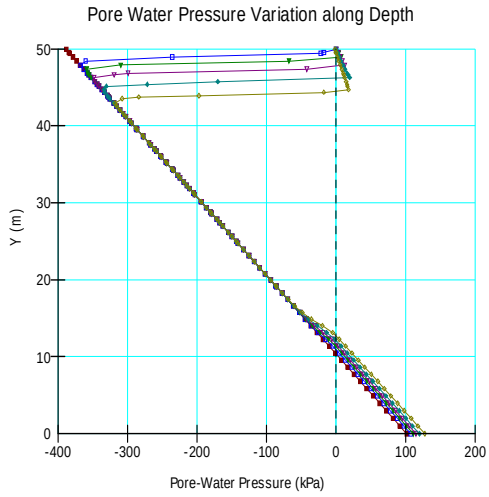

(a) Section 1-1

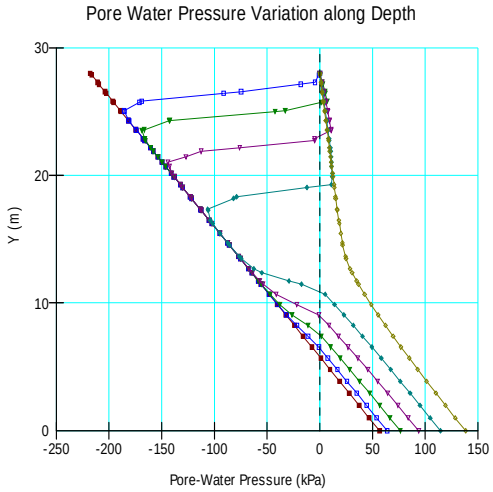

(b) Section 2-2

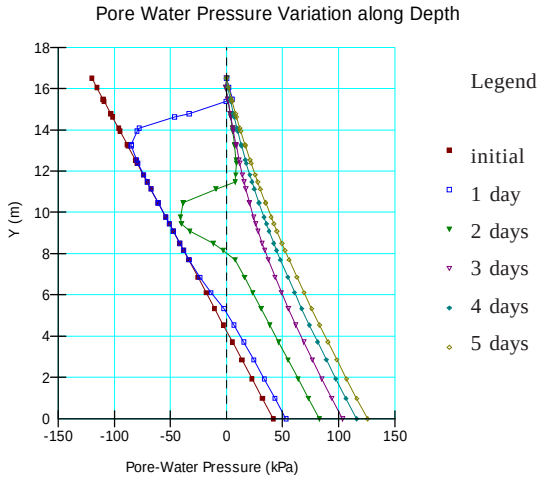

(c) Section 3-3

Figure 8: Results of 20mm/hr Rainfall for Case 1

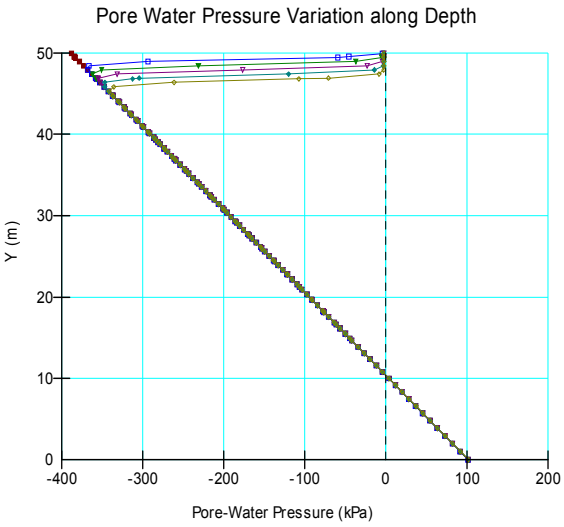

(a) Section 1-1

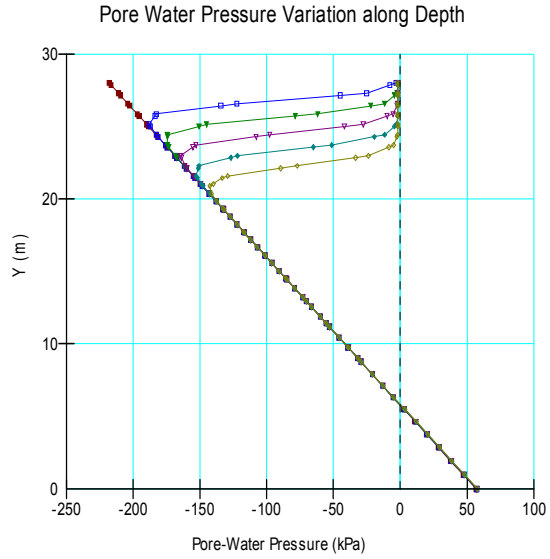

(b) Section 2-2

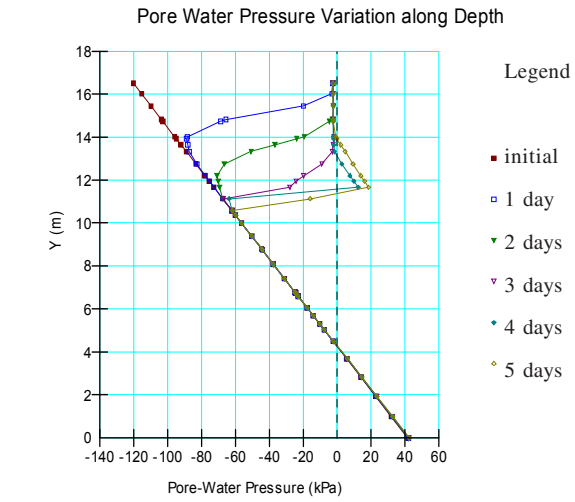

(c) Section 3-3

Figure 9: Results of 05mm/hr Rainfall for Case 2

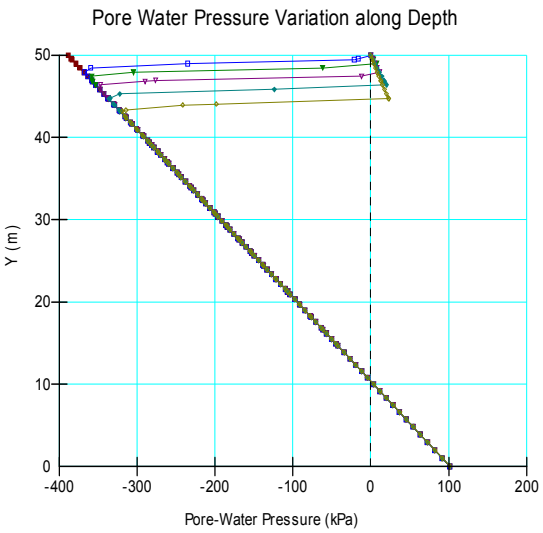

(a) Section 1-1

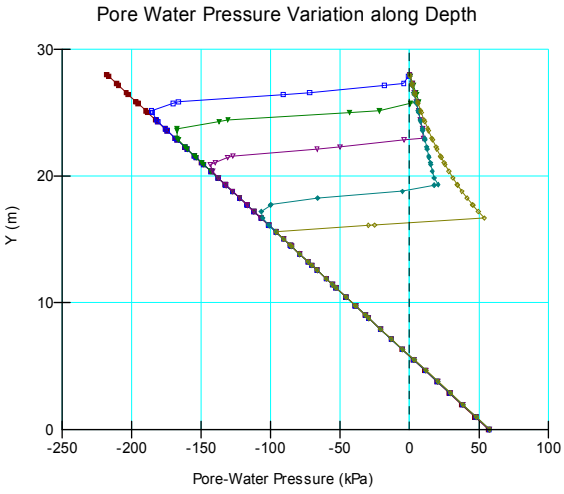

(b) Section 2-2

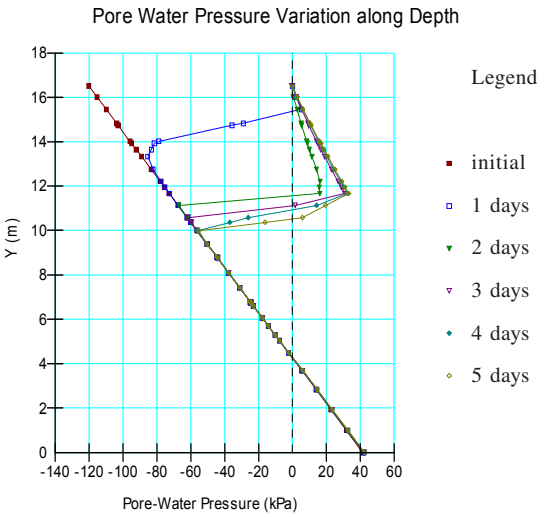

(c) Section 3-3

Figure 10: Results of 20mm/hr Rainfall for Case 2

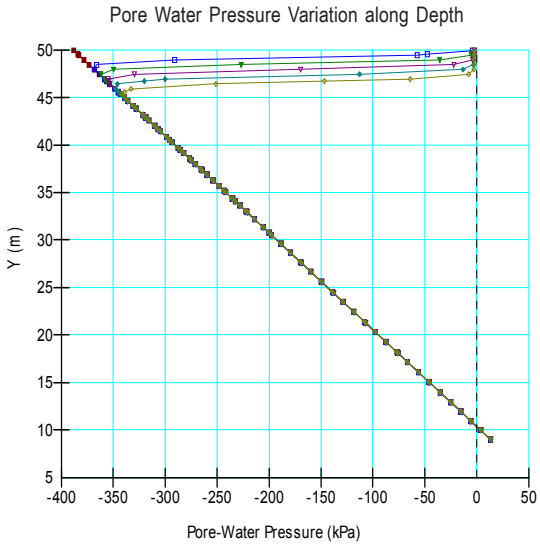

(a) Section 1-1

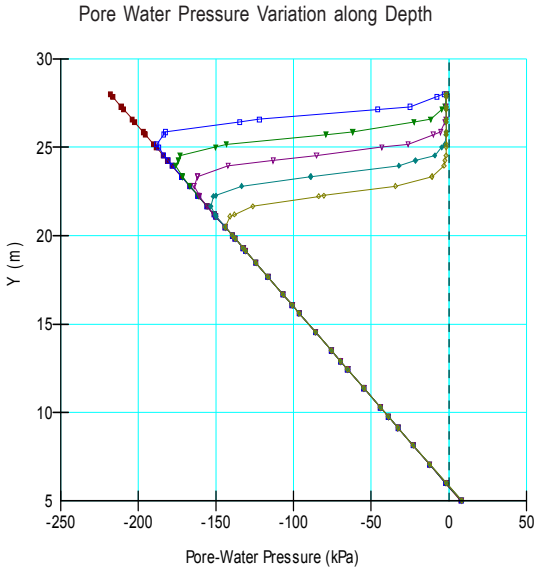

(b) Section 2-2

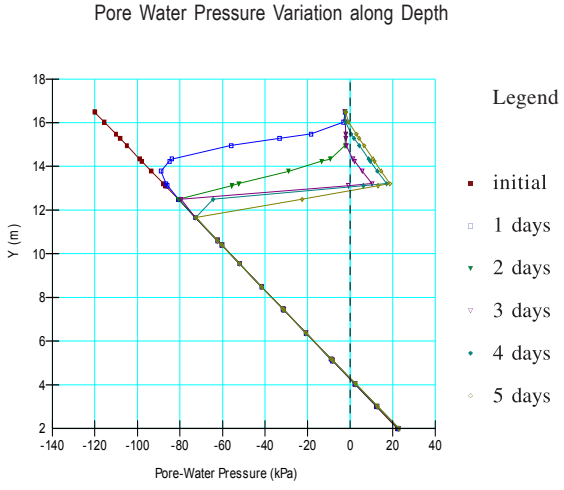

(c) Section 3-3

Figure 11: Results of 05mm/hr Rainfall for Case 3

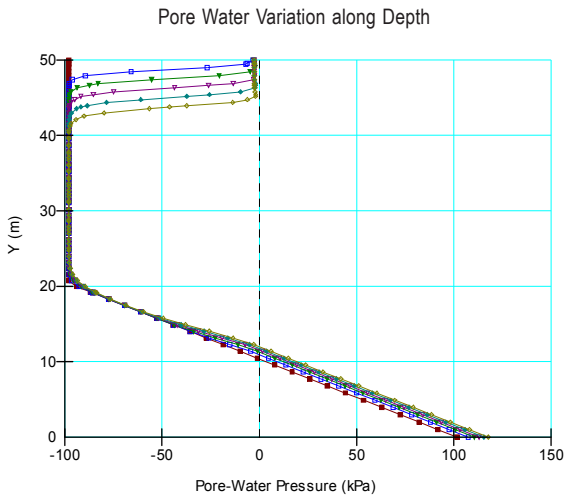

(a) Section 1-1

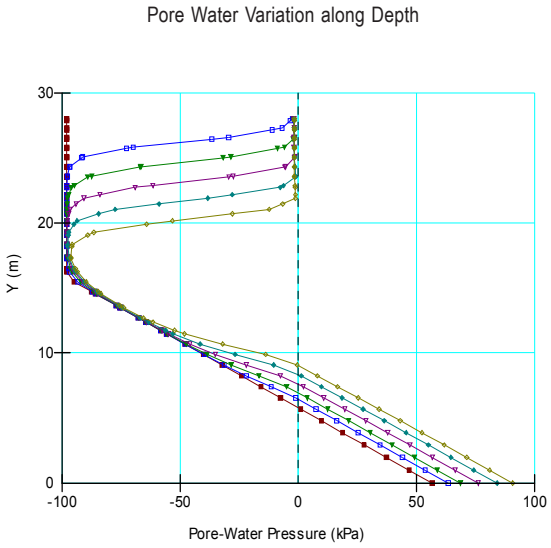

(b) Section 2-2

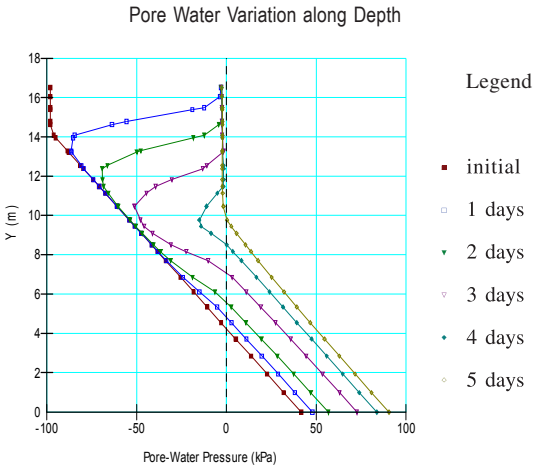

(c) Section 3-3

Figure 12: Results of 05mm/hr Rainfall for Case 1

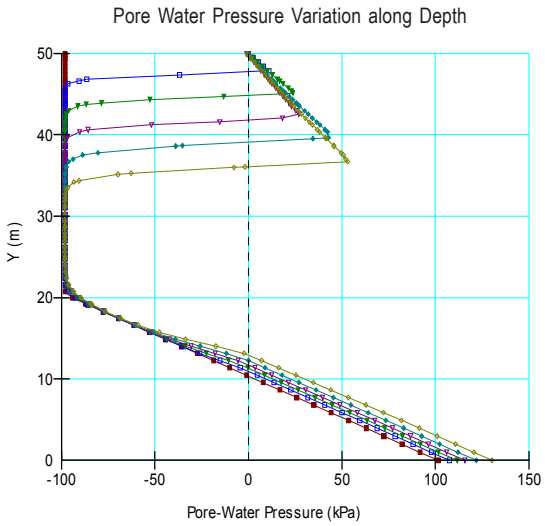

(a) Section 1-1

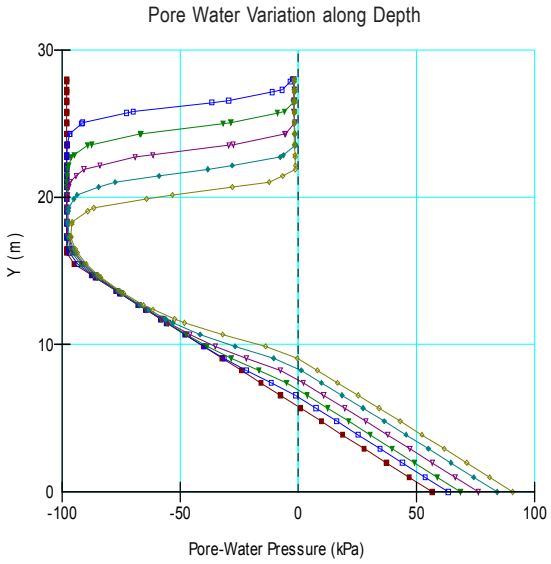

(b) Section 2-2

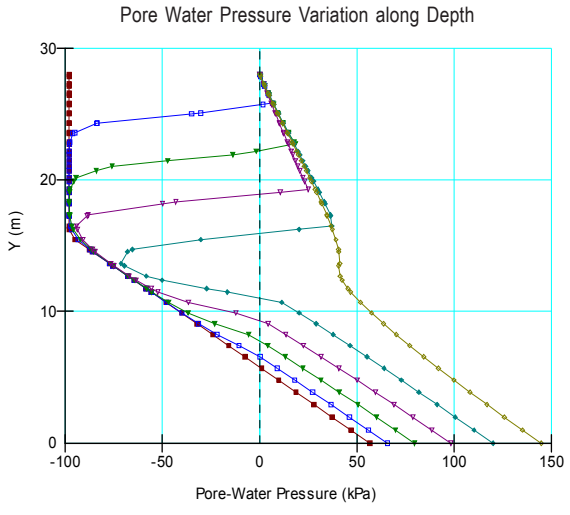

(c) Section 3-3

Figure 13: Results of 20mm/hr Rainfall for Case 1

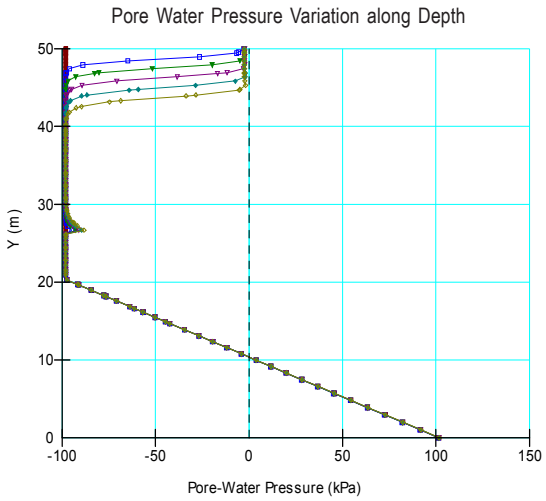

(a) Section 1-1

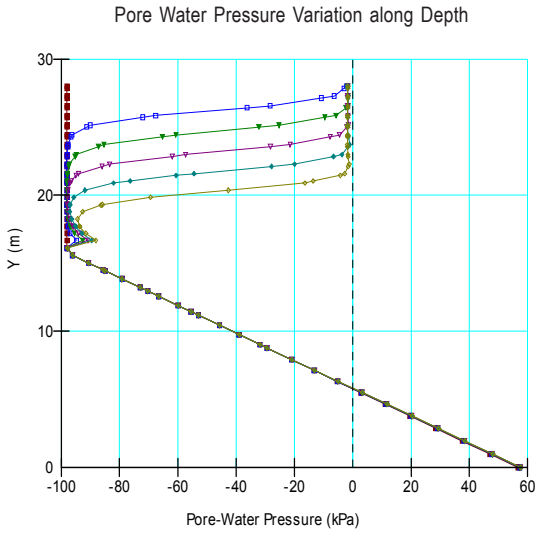

(b) Section 2-2

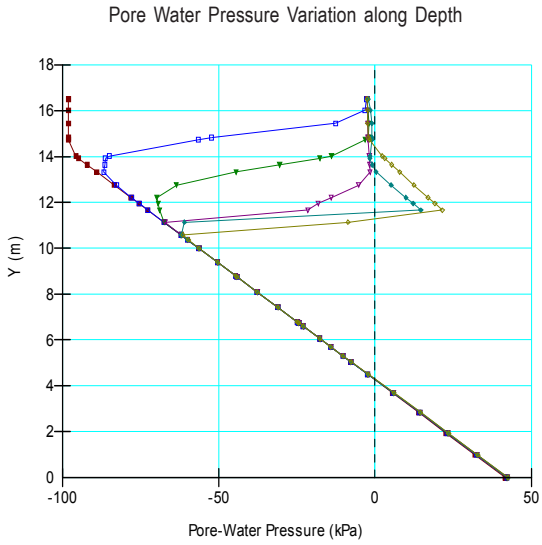

(c) Section 3-3

Figure 14: Results of 05mm/hr Rainfall for Case 2

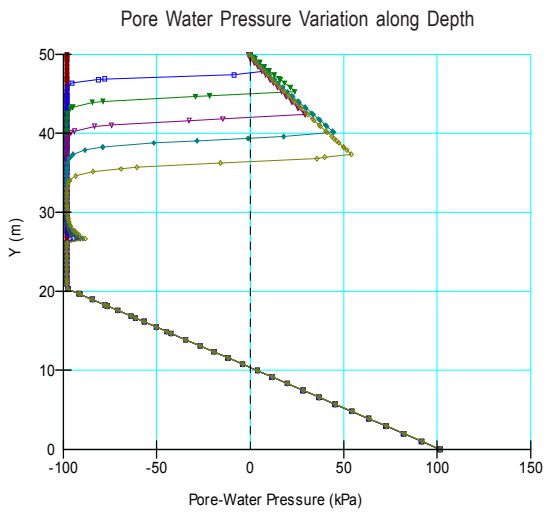

(a) Section 1-1

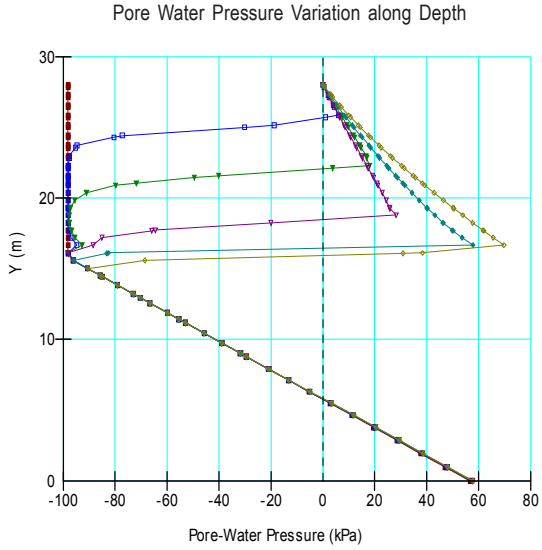

(b) Section 2-2

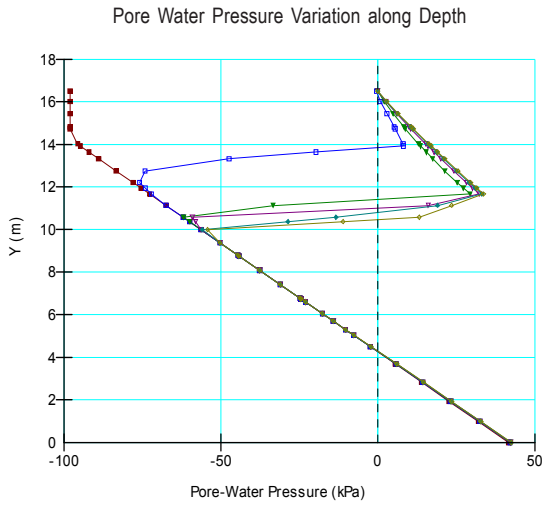

(c) Section 3-3

Figure 15: Results of 20mm/hr Rainfall for Case 2

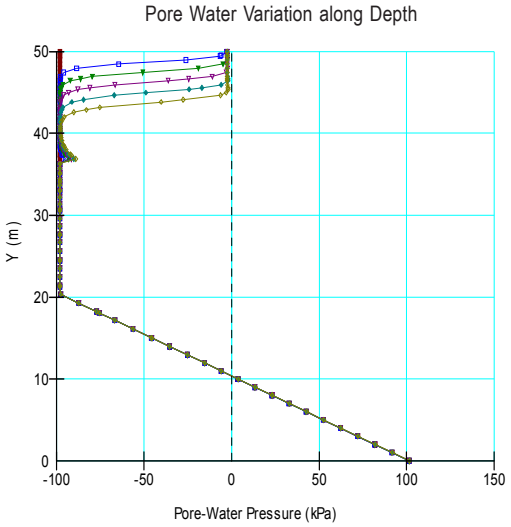

(a) Section 1-1

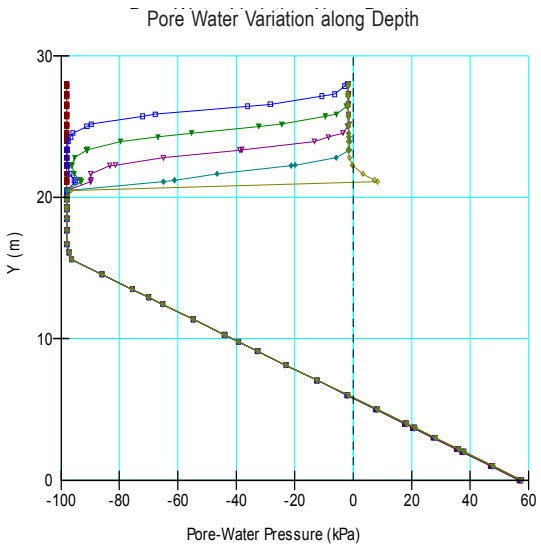

(b) Section 2-2

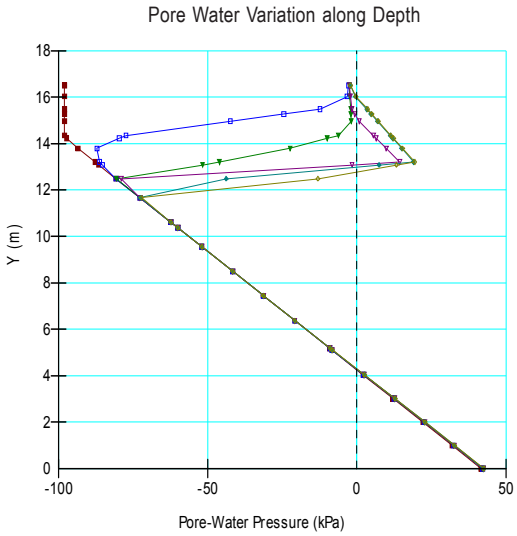

(c) Section 3-3

Figure 16: Results of 05mm/hr Rainfall for Case 3

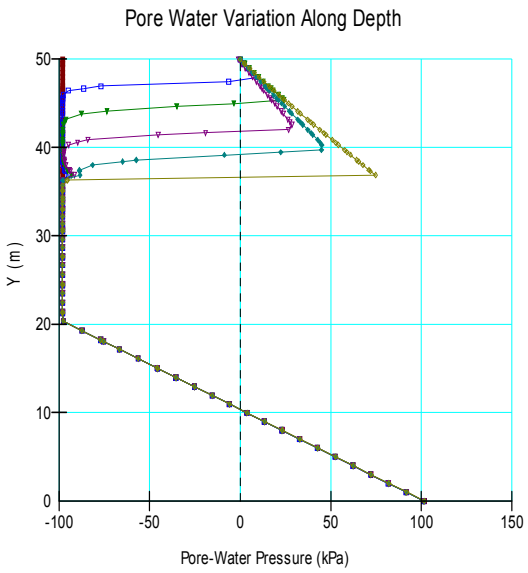

(a) Section 1-1

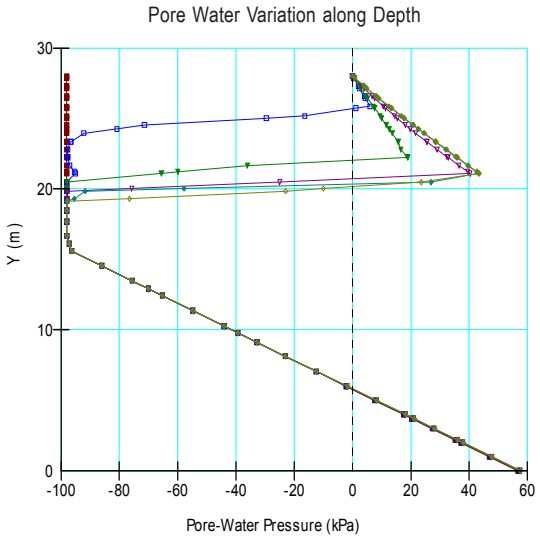

(b) Section 2-2

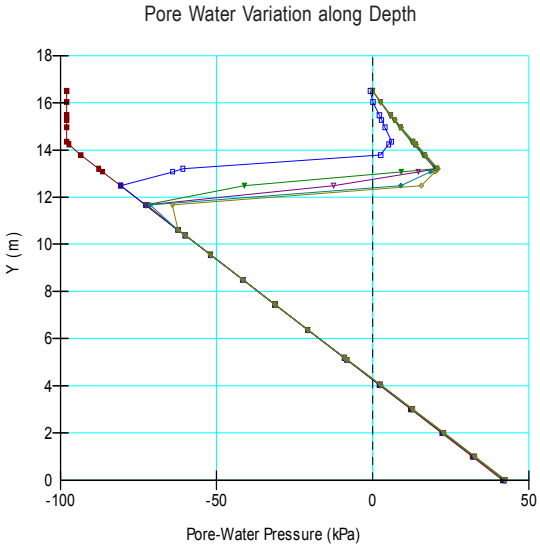

(c) Section 3-3

Figure 17: Results of 20mm/hr Rainfall for Case 3

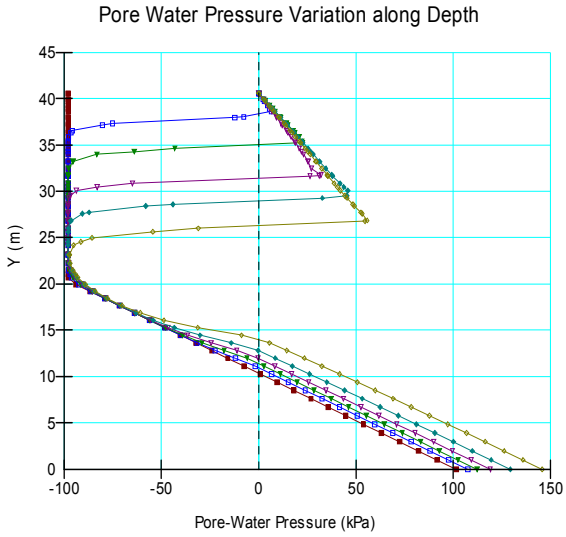

(a) Section 1-1

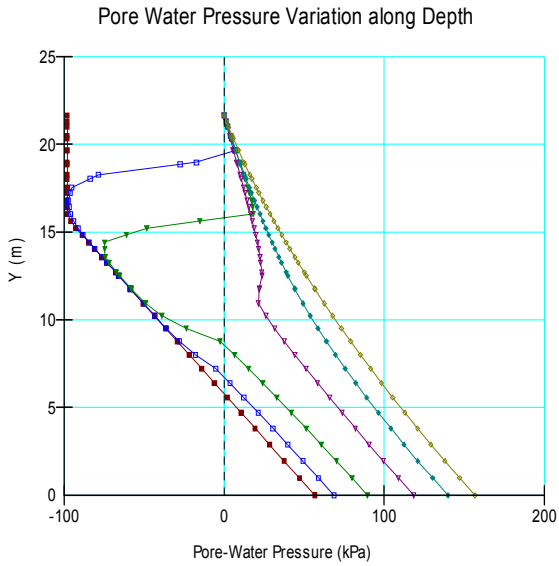

(b) Section 2-2

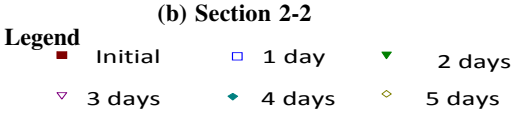

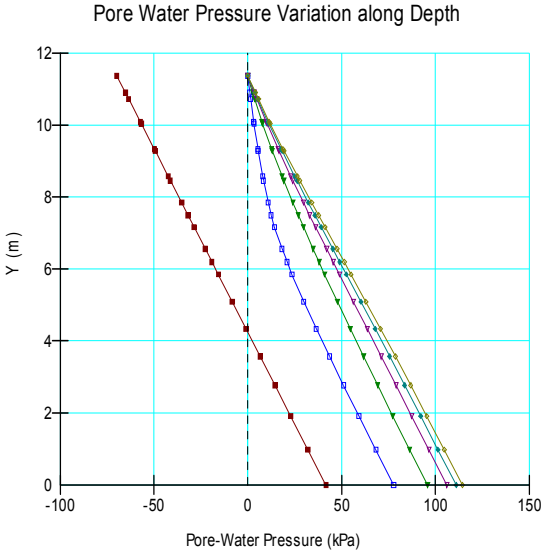

(c) Section 3-3

Figure 18: Results for 20mm/hr rainfall for case 1 in slope cut to 1:1.267

boundary of the two layers in Section 1-1 and section 2-2 in Figure 14. For a rainfall for an intensity 20 mm/hr, larger positive pore water pressures were developed extending to a greater depth down to the boundary of the two layers.

For Case 3, where the thickness of the residual soil layer was smaller, a rainfall of intensity 5 mm/hr caused the development of larger positive pore water pressures over the lower sections. The development of perched water table near the boundary was more prominent than for the Case 2. (Figure 16).

With a heavier rainfall of intensity 20 mm/hr, positive pore water pressures have developed even at the upper sections. 1-1 and 2-2) (Figure 17).

(c) Response of cut slope with a gradient of 1:1.267

Similar series of analyses were done for the slope cut to a gradient of 1:1.267. Results of the analysis corresponding to a rainfall of intensity 20mm/hr under the conditions of Case 1 are presented in Figure 18. These plots should be compared with Figure 13. The comparison shows that with the flatter slope losses in matric suction were greater. This could be attributed to the greater amount of infiltration that occurred over a wider surface area.

Conclusion

Landslides in Sri Lanka are triggered by excessive rainfall. This is a scenario common to many countries with a tropical climate. Deforestation and unplanned development in view of providing facilities demanded by the rapid development has aggravated the situations.

As such, it is very important in the present day context to understand clearly the mechanisms of rain induced slope failures, so that, preventive actions can be taken before a catastrophe.
Sri Lankan slopes are made of residual soil and upper parts of them are in unsaturated state during the periods of dry weather. High matric suction that prevails in the unsaturated zone of the soil enhances the stability of the slope. As such, very steep and high slopes could be seen stading safe. This research done with SEEP/W –(2007) illustrated how the infiltration of rainwater destroys the matric suction and cause the rise of ground water table as rainfall prolongs. The destruction of the matric suction commences at the surface and the wetting front progresses downwards as rainfall continues. The water infiltrated downward will cause a rise of the level of the ground water table. Towards the toe of the slope the infiltration would give rise to development of positive pore water pressures.

Increase of rainfall intensity to a level comparable with the saturated permeability of the soil, will cause further progression of the wetting front and the rise of the ground water table. Beyond a certain value the excessive rainfall will contribute to runoff.

If a layer of less weathered material is present beneath the residual soil, the low permeability of that material will inhibits the infiltration. As a result water would pond at the boundary of the two layers of contrasting permeability leading to the formation of a perched water table. With rainfalls of greater intensity much higher positive pre water pressures would develop in the more permeable upper layer. As such, the presence of a less weathered highly impermeable layer of material at a shallow depth would have a negative effect on the stability of the slope.

References

Fredlund, D. G., and Rahardjo, H. (1993). *"Soil mechanics for unsaturated soils"*, Wiley, New York.

Fredlund, D. G., Xing, A. and Huang, S. Y. (1994)." Predicting the Permeability Function for Unsaturated Soils Using the Soil-Water Characteristic Curve, Canadian Geotechnical Journal Vol 31, pp 533-546.

GEO-SLOPE International Ltd. (2007)" "Seepage Modeling with SEEP/W 2007-An Engineering Methodology" *Calgary, Alberta, Canada*, Second Edition, May 2007

Mukhlisin.M and Raihan.M.T (2008) "Effect of Antecedent Rainfall on Slope Stability at a Hill slope of Weathered Granitic Soil Formation" *International Conference on Slopes, Malaysia 2008.*

Sun.H.W, Wong. H.N and Ho. K.K.S (1998) "Analysis of infiltration in unsaturated ground", *Slope Engineering in Hong Kong, Li, Kay & Ho(eds)*© 1998 Balkema, Rotterdam, ISBN 90 5410935 1.

Kulathilaka S.A.S[1] and Sujeevan V[2]

Rain Triggered Slope Failures in Unsaturated Residual Soils

ABSTRACT: This paper is a continuation of the research paper titled "Rainfall Infiltration Analysis in Unsaturated Residual Soil slopes", which discussed the changes in the pore pressure regime of a slope made of unsaturated residual soils, due to prolonged rainfall. This paper discusses the consequent changes in the safety margins of the slope.

Residual soils, which remain at the location of the parent rock after weathering are characterized by different degrees of weathering, difference in the weathered product based on the mineralogical composition of the parent rock and significant variations within a short distance due to above reasons. Zones of different levels of weathering will have significantly different hydraulic and shear strength properties.

Rain induced slope failures are a common geotechnical problem in the tropics. In this study the complex geological situations in a residual soil slope is idealized by two states; a uniform soil slope and a slope of weathered rock underlying the soil. Two typical cut slopes from the Southern Transport Development Project were used in the analysis.

The variation in the safety margins of the slope with the progression of the rainfall was analyzed by the Bishop's simplified method and the Spencer's method. The analysis was done with the SLOPEW computer software and the data on the changes of the pore pressure regime computed with SEEPW analysis were incorporated. Initially, the safety margins were assessed through the computation of factor of safety and subsequently a probabilistic analysis was done accounting for the uncertainties in the properties of soil such as, friction angle, cohesion, and pore water pressure. Monte-Carlo approach was used in the probabilistic analysis.

Key Words

Slope stability; Residual soils; Matric suction; Rainfall; Unsaturated soil; Probabilistic analysis

Background

Rainfall-induced slope failure constitutes one of the most common geotechnical hazards in tropical regions such as Sri Lanka. Landslides in residual soils are often triggered by prolonged extensive rainfalls. Conditions leading to these failures are caused by the loss of matric suction and rise in pore-water pressure as a result of infiltration of rainwater. Infiltration into soils depends on several factors such as soil structure, antecedent soil moisture, soil exchangeable medium, infiltrating water quality, and the status of the soil air. This aspect was discussed in the companion paper.

The objective of the research presented in this paper is to study how the infiltration process affect the stability of the slope consequently. Safety was assessed in terms of both the factor of safety and the probability of failure.

Methodology

The analysis was performed on two typical cut slopes in the southern expressway project. Considering the highly variable conditions encountered, three different sub soil conditions were studied in the project. The Case 1 was a slope made of a uniform residual soil. In Case 2 a less weathered layer - weathered rock- is underlying the thick residual soil layer. In Case 3 a less weathered layer is underlying a thin residual soil layer. The weathered rock layer is with greater shear strength and lower permeability. This is a very broad simplification of the situation seen in many slopes in the country. In reality the degree of weathering could change abruptly and presence of relit discontinuities will add further complications. Analyses were performed on cut slopes of two different gradients; 1:1 and 1:1.267.

After the infiltration analysis, the stability of the slope was analyzed using the SLOPE/W-2007 *(GEO-SLOPE International Ltd. -2007)* package incorporating the pore water pressures derived from the SEEP/W analysis. Stability analyses were carried out for different time steps ranging from 1 day to 5 days for rainfalls of intensity 5mm/hr, 20mm/hr and 40 mm/hr respectively. Initially, the values of factor of safety were computed and subsequently the probability of failure was evaluated.

Considering the possibility of occurrence of both circular and non circular modes of failure, Bishop's simplified method and Spencer's method were used in the analysis. Analyses were done only for the first time failures. As such, peak shear strength parameters were used in the study.The probabilistic analysis was done with the Monte-Carlo formulation.

Saturated and Unsaturated Soils

All the voids in a soil below the ground water table are filled with water and the soil is in a saturated state. Above the ground water table some voids are filled with air and the soil is in an unsaturated state and a three phase system exists with solids, water and air. Consequently both pore water pressure (u_w) and pore air pressure (u_a) should be considered in an analysis. The pore air pressure is usually equal to the atmospheric. The pore water pressure above ground water table is less than atmospheric and the variation is presented in a simplified form as full line in Figure 1. Providing a limit to the practically possible maximum matric suction, a more realistic distribution is presented in broken lines in Figure 1. Two stress variables σ-u_a termed net normal stress and (u_a-u_w) termed matric suction are used in the analysis.

This figure corresponds to the condition of the slope during a period of dry weather. Modifications in the pore pressure regime due to the infiltration of rainwater were discussed in detail on the companion paper.

[1]**Professor, Department of Civil Engineering, University of Moratuwa, Sri Lanka**

[2]**Ph.D Student, University of Southampton,England**

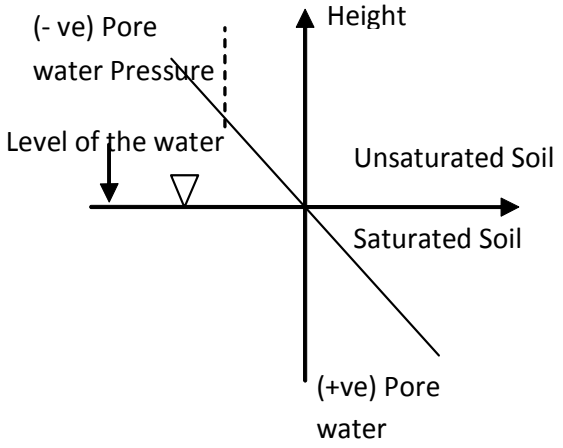

Figure 1: Pore water pressure distribution

Shear Strength of Unsaturated Soil

Shear strength equation as applied for unsaturated soils will be used in this research for the slope stability analysis to incorporate the contribution from the negative pore-water pressure. The equation for unsaturated shear strength is given by; *(Fredlund et al. 1978).*

$$\tau = c' + (\sigma_n - u_a)\tan\phi' + (u_a - u_w)\tan\phi^b \quad - \quad 01$$

Where τ-shear strength of unsaturated soil; *c'*-effective cohesion intercept; ($\acute{o}_n - u_a$) - net normal stress; $\acute{o}_n$ -total normal stress; u_a – pore-air pressure; ϕ' – effective angle of shearing resistance; (u_a-u_w) -matric suction; u_w-pore-water pressure; and ϕ^b – angle indicating the rate of increase in shear strength relative to the matric suction. The shear strength given by *Equation-01* is intended for linear failure envelope.

Under the unsaturated conditions the apparent cohesion term can be expressed as:

$$c_a = c' + (u_a - u_w)\tan\phi^b \quad - \quad 02$$

Limit equilibrium Approach

In the limit equilibrium approach of assessing the stability of a slope, factor of safety values are determined for a number of assumed trial failure surfaces. The lowest of the value obtained is taken as the factor of the slope and corresponding failure surface is the critical failure surface.

The factor of safety (*F*) is defined as;

$$F = \frac{\tau_f}{\tau_m} \quad - \quad 03$$

Where τ_f = Shear Strength

$$= c' + (\sigma_n - u_a)\tan\phi' + (u_a - u_w)\tan\phi^b$$

τ_m = Shear strength mobilized for equilibrium.

Equilibrium of the failure mass should be considered in obtaining the factor of safety value. In the methods of slices, the failure mass is divided in to number of vertical slices. There are number of different methods of slices based on the assumptions made to make the system of forces statically determinate.

Bishop's Simplified Method of Slices

Bishop's simplified method is widely used in practice to analyze circular failure surfaces. This method considers the interslice normal forces but neglects the interslice shear forces. In Bishops simplified method of slices, the mode of failure has to be rotational and the failure should be an arc of a circle. It satisfies only the moment equilibrium. A comparison with the other rigorous methods satisfying both force and moment equilibrium has shown that the maximum error in the factor of safety given by the Bishop's simplified method for circular failure surfaces is within 8%. *(Krishna et.al-2006))*

In the SLOPE/W(2007) program, Bishop's simplified method was formulated to include both negative and positive pore water pressures computed from the infiltration analysis. The data on pore water pressure could be directly imported to SLOPEW program from the SEEPW program.

Spencer's Method

Spencer's method assumes that the side forces are parallel, i.e., all side forces are inclined at the same angle. Spencer's method also assumes that the normal forces on the bottom of the slice act at the center of the base – an assumption which has very little influence on the final solution. Spencer's Method fully satisfies the requirements for both force and moment equilibrium.

Although Spencer originally presented his method for circular slip surfaces, later it was shown that the method could readily be extended to analyses with noncircular slip surfaces. A solution by Spencer's method first involves an iterative, trial and error procedure in which values for the factor of safety (F) and side force inclination are assumed repeatedly until all conditions of force and moment equilibrium are satisfied for each slice.

Spencer's Method requires computer software to perform the calculations. Because moment and force equilibrium must be satisfied for every slice and the calculations are repeated for a number of assumed trial factors of safety and interslice force inclinations. Complete and independent hand-checking of a solution using Spencer's Method is impractical *(US Army Corps of Engineers -2003)*. Spencer's method was used in this research to analyze non circular mode of failure surfaces.

Modes of Trial Failure Surfaces

Circular Shaped slip surfaces

Circular shape failure surfaces are observed in relatively homogeneous materials. A circular slip surface is easier to analyze, because it is convenient to sum moments about the center of the circle. A circular slip surface must be used in the Ordinary Method of Slices and Simplified Bishop Method. Also, circular slip surfaces are generally sufficient for analyzing relatively homogeneous embankments or slopes and embankments on foundations with relatively thick soil layers.

Wedge shaped slip surfaces

Wedge shaped failure mechanisms are defined by three straight line segments defining an active wedge, central block, and passive wedge. This type of slip surface may be appropriate for slopes where the critical potential slip surface includes a relatively long linear segment through a weak material bounded by stronger material. A common example is a relatively strong levee embankment founded on weaker, stratified alluvial soils.

General Non-circular Slip Surfaces

This is also called the optimized slip surface. General, non circular shape Slope failure may occur by sliding along surfaces that do not correspond to either the wedge or circular shapes. The term general slip surface refers to a slip surface composed of a number of linear segments which may each be of any length and inclined at any angle. The term "noncircular" is also used in reference to such general-shaped slip surfaces. Prior to about 1990, slip surfaces of a general shape, other than simple wedges, were seldom analyzed, largely because of the difficulty in systematically searching for the critical slip surface. However, in recent years improved search techniques and computer software have increased the capability to analyze such slip surfaces. Stability analyses based on general slip surfaces are now much more common and are useful as a design check of critical slip surfaces of traditional shapes (circular, wedge) and where complicated geometry and material conditions exist. It is especially important to investigate stability with noncircular slip surfaces when soil shear strengths are anisotropic.

A number of techniques have been proposed and used to locate the most critical general-shaped slip surface. One of the most robust and useful procedures is the one developed *by* Celestino and Duncan (1981).In this method, an initial slip surface is assumed and represented by a series of points that are connected by straight lines. The factor of safety is first calculated for the assumed slip surface. Next, all points except one are held fixed, and the "floating" point is shifted a small distance in two directions. The directions might be vertically up and down, horizontally left and right, or above and below the slip surface in some assumed direction. The factor of safety is calculated for the slip surface with each point shifted as described. This process is repeated for each point on the slip surface. As any one point is shifted, all other points are left at their original location. Once all points have been shifted in both directions and the factor of safety has been computed for each shift, a new location is estimated for the slip surface based on the computed factors of safety. The slip surface is then moved to the estimated location and the process of shifting points is repeated. This process is continued until no further reduction in factor of safety is noted and the distance that the shear surface is moved on successive approximations becomes minimal. *(US Army Corps of Engineers -2003)*

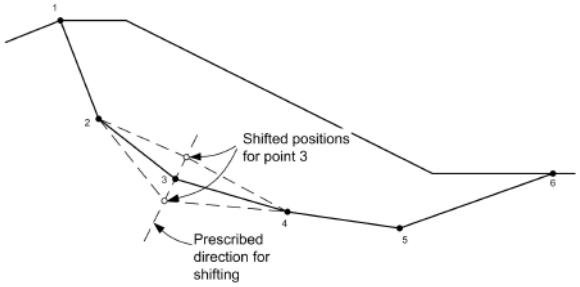

Figure 2: Search scheme for noncircular slip surfaces (after Celistono and Duncan 1981)

Probabilistic Analysis

Deterministic slope stability analyses compute the factor of safety based on a fixed set of conditions and material parameters. If the factor of safety is greater than unity, the slope is considered to be stable. On the contrary, if the factor of safety is less than unity, the slope is considered to be unstable or susceptible to failure. Deterministic analyses suffer from limitations that the variability of the input parameters is not considered. Probabilistic slope stability analysis allows for the consideration of variability in the input parameters that possess some degree of uncertainty and it quantifies the probability of failure of a slope.

Pore pressure, cohesion and friction angle, and friction angle indicating the rate of increase in shear strength relative to the matric suction are treated as uncertain parameters and the other soil parameters such as density which are less variable and parameters related to geometry are treated as deterministic. The probability of failure is defined as the probability the FOS is less than the unity. This is expressed as factor or a percentage.

Uncertainties in the shear strength parameters and pore water pressures used could be accounted for in a probabilistic analysis. The mean values and the standard deviations given in Table 1 are used in the analysis. In this research probabilistic analysis was performed using the Monte-Carlo approach, a facility available in the SLOPE/W program. Here the stability analyses were conducted thousands of time varying the parameters within a range based on the mean value and the standard deviation. Using the large number of FOS values computed in this analysis, the probability the FOS would be less than 1.0 is computed and referred to as the probability of failure.

If the probability of occurrence of 5mm/hr or 20mm/hr rainfall can be obtained using available data, an annual probability of failure, A p(f) could be computed by;
A p(f) = p(f-SLOPEW) ´ p(occurrence of rainfall)

Decision regarding (remedial measures to be adopted) can be taken based on the annual probability of failure.

Slope Stability Analysis Using SLOPE/W

Infiltration of rainwater through an unsaturated zone results in the formation of a wetted zone and a destruction of matric suction near the slope surface. This loss of matric suction would reduce the apparent cohesion and may lead to failure during periods of prolonged rainfall. These failures are usually characterized by shallow failure surfaces that develop parallel to the slope surface.

With the loss of matric suction and development of positive pore water pressures over shallow depths, the potential failure surface could be non-circular. This aspect was considered in the analysis of the stability of the slope that was done through the limit equilibrium approach. Circular mode of failures was analyzed through the Bishop's simplified method and non-circular modes of failure were analyzed through the Spencer's method.

The minimum factor of safety and the corresponding most critical failure surface at different times into the rainfall were obtained using through the analysis. Soil shear strength parameters used in the slope stability analysis are given in Table 1

	Unit Weight (γ_{eff})	Friction angle (ϕ')	(ϕ^b)	(c')
Residual Soil				
Mean	19	34	30	10
S Deviation	0.5	1.5	2	1.5
HWR				
Mean	20	40	38	25
S Deviation	0.5	1.5	2	1.5

Table 1: Soil strength parameters used for stability analysis and standard deviations

Slope Geometry Used

The geometry of typical cut slopes used for the stability analysis are shown in Figure 3 and Figure.4. In the homogeneous soil (Case 1) the entire slope is made of residual soils and in the Case 2, there is a layer of residual over weathered rock. In Case 3, the thickness of the residual soil layer is smaller. The figure corresponds to case 3. The boundary between the two soils is shown by line AB in Figure 3. Two slope geometries; one with cut slope gradient of 1:1 with intermediate berms (Figure 3) and another with cut slope gradient of 1:1.267 with intermediate berms. (Figure 4), used in the infiltration study were used for the stability analysis as well.

Results of Deterministic Stability Analysis

Slope cut to a 1:1 gradient

For the slope cut to a gradient of 1:1, the variation of the factor of safety with the progression of the rainfall was analyzed incorporating the data from the infiltration analysis. The analyses were done for the cases of uniform slope (Case 1), thick layer of residual soil overlying weathered rock (Case 2) and thin layer of residual soil overlying weathered rock (Case 3). The results obtained with the assumption of the initial matric suction profile 1 are presented in Figure 5. The results obtained with the assumption of a matric suction profile with an upper limit are presented in Figure 6. The reduction of the factor of safety with the progression of the rainfall is evident from both figures.

Figure 3: Typical Cut Slope Geometry - 1:1 cut slope

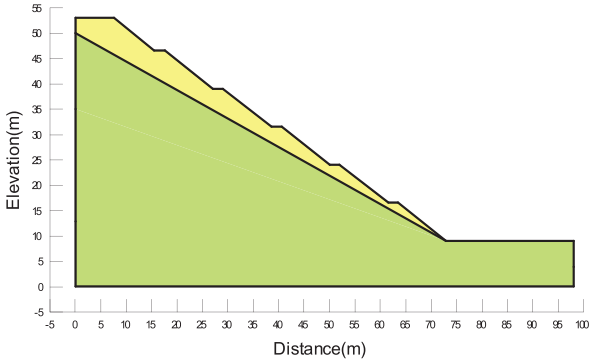

Figure 4: Typical Cut Slope Geometry - 1:1.267 cut slope

It is also evident that although the two layered slope had a greater factor of safety during the dry stages, the factor of safety reduced rapidly as rainfall continued. This is due to the built up of positive pore water pressures in the more permeable upper layer as the restriction for downward flow are imposed by the weathered rock layer of much lower permeability. This aspect was well illustrated in the infiltration analysis. The reduction of factor of safety was more rapid for the rainfall of greater intensity 20mm/hr. For the homogeneous slope the factor of safety approached unity after 3 days of 20mm/hr rainfall. But with the two layered soil this event took place only after 2 days.

Infiltration analysis showed that, when an upper limit of 100kN/m^2 was imposed on the matric suction profile, a greater loss of matric suction and greater positive pore water pressures were developed for rainfall of given intensity. This effect was reflected in the stability analysis. As presented in Figure 7, the factor of safety decreased more rapidly when there was an upper limit of 100kN/m^2 was imposed for the initial matric suction.

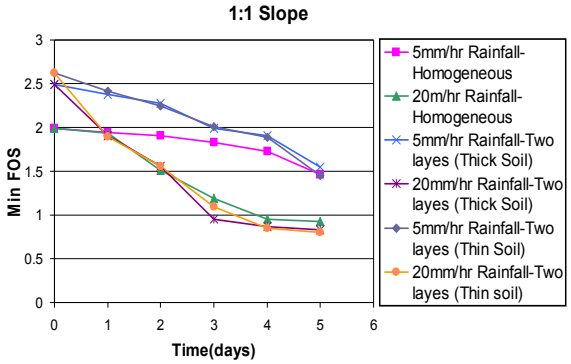

Figure 5: Variation of factor of safety with duration of rainfall – maric suction profile 1

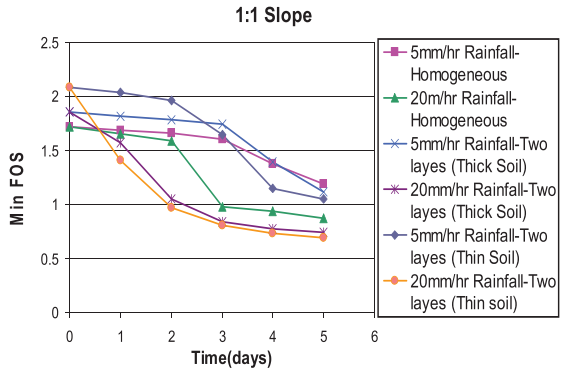

Figure 6: Variation of factor of safety with duration of rainfall - maric suction profile with an upper limit

The differences in the shape of the critical failure surfaces corresponding to the different durations of the rainfall should also be noted. At the initial stages of the rainfall or during the dry season, the presence of high matric suctions near the surface induces greater shear strength in the soils. As such, critical failure surfaces are quite deep. The critical failure surfaces for the homogeneous slope and the two layered slope at the initial stages are presented in Figure 7 and Figure 8 respectively.

As rainfall occurs the loss of matric suction and development of positive pore water initiates near the surface and progresses

downward with time. The greatest effect on the reduction of shear strength is closer to the ground surface. As such, the critical failure surfaces corresponding to the latter stages are much shallower as illustrated by Figure 9 and Figure 10 for the uniform slope and two layered slope respectively.

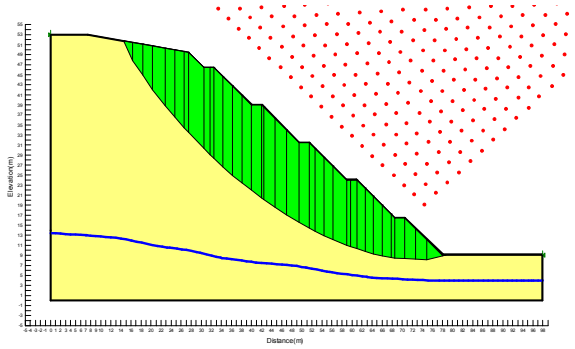

Figure 7: Shape of typical failure surface - homogeneous soil slope at initial stage

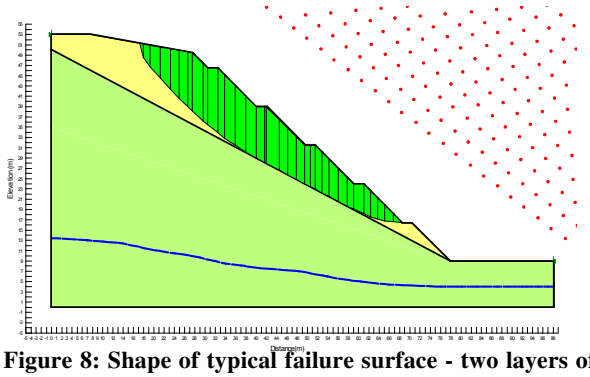

Figure 8: Shape of typical failure surface - two layers of soil slope at initial stage

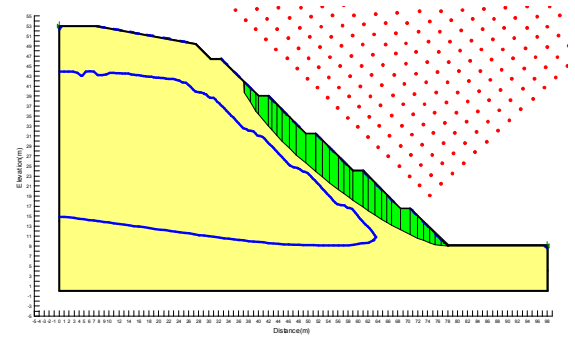

Figure 9: Shape of typical critical failure surface – homogeneous slope at a later stage

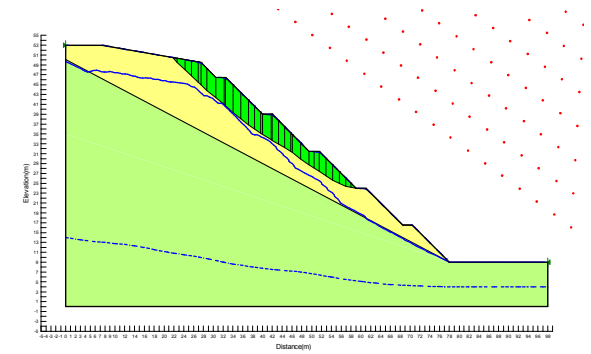

Figure 10: Shape of typical critical failure surface -two layers of soil at a later stage

Slope cut to a 1:1.267 gradient

There is a general perception that when a slope is cut to a flatter angle it would possess a greater factor of safety. This is certainly true for many situations, but the effect of rainfall on the much wider area resulting from the flatter angle of cut should be carefully studied. As such, the effect of rainfall on the pore pressure regime of a slope cut to a gradient of 1:1.267 was studied. Studies were done for homogeneous slope (Case 1), slope with a thick layer of residual soil (Case 2) and slope with a thin layer of residual soil (Case3). Infiltration study was done for both initial matric suction profiles. Thereafter, stability analysis was done incorporating the changes in the pore pressure regime. The variation of the factor of safety with the duration of rainfall for the initial pore pressure profile 1 is presented in Figure 11 for Case 1, Case 2 and Case 3 for 5mm/hr and 20 mm/hr rainfalls. For the assumption of the initial matric suction profile with an upper limit, the variation of factor of safety with the duration of the rainfall is presented in Figure 12.

Variation of the factor of safety for the 1:1 slope and 1:1.267 slopes in homogeneous soil for the assumed matric suction profile 2, is compared in Figure 13. It clearly shows that although the 1:1.267 slope has a much greater factor of safety at the start of the rainfall, after 3 days of rainfall its factor of safety is similar to that corresponding to the 1:1 slope. As such, it is clear that if proper drainage measures are not adopted, making the slope flatter alone would not ensure safety.

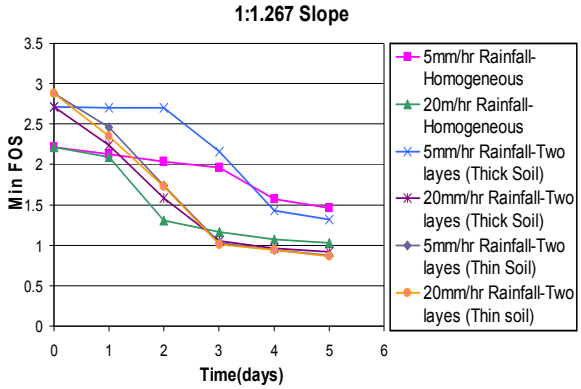

Figure 11: Variation of factor of safety with duration of rainfall – 1:1.267 slope with maric suction profile 1

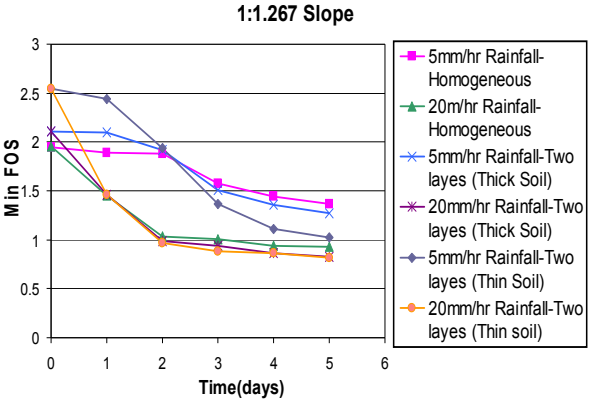

Figure 12: Variation of factor of safety with duration of rainfall –1:1.267 slope with maric suction profile with an upper limit

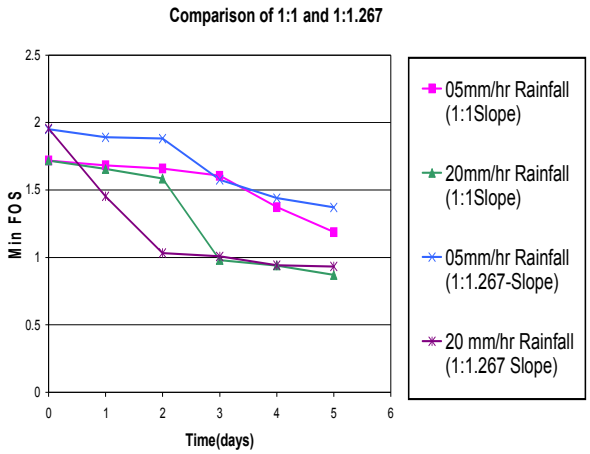

Figure 13: Comparison factor of safety – slopes of 1:1 and 1:1.267 with uniform soil – maric suction profile 1

Time	0	1	2	3	4	5
5mm/hr Homogeneous Slope	0	0	0	0	0	0.15
20mm/hr Homogeneous Slope	0	0	0	53.13	92.44	99.40
05mm/hr Two Layers (Thick layers)	0	0	0	0	0	2.10
05mm/hr Two Layers (Thick layers)	0	0	18.90	100	100	100
05mm/hr Two Layers (Thin layer)	0	0	0	0	0.70	18.60
20mm/hr Two Layers (Thin layer)	0	0	67.55	100	100	100

Table2: Probability of failure for 1:1 slope

Results of Probabilistic Analysis

By using the Monte-Carlo approach the minimum factor of safety values are calculated in each random value of soil properties. Then the software SLOPE/W 2007 automatically plots the probability density function. A typical probability density function is presented in Figure 14. It corresponded to the two layered soil (Case 3) and rainfall of intensity 20 mm/hr.

Probability density functions were found in each time step. In a Probability density function, the percentage probability of failure is given by the area corresponding to FOS<1.

The values of percentage probability of failure under different sub soil conditions, for the 1:1 cut slope with the assumption of matric suction profile 2 (with an upper limit) are presented in Table 2. The values of percentage probability of failure for the cut slope of 1:1.267 gradient under similar conditions are presented in Table 3.

The increase of the probability of failure with the progression of the rainfall is clearly evident from the data in the tables. It is also evident that the two layered slope (Case 3) is more vulnerable than the uniform slope. The probability of failure increased with the intensity of the rainfall.

With rainfall, the probability of failure of the slope cut to a gradient of 1:1.267 increased more rapidly than in the case of the slope cut to 1:1 gradient.

Time (Days)	0	1	2	3	4	5
5mm/hr Homogeneous Slope	0	0	0	0	0	0
20mm/hr Homogeneous Slope	0	0	28.0	42.90	86.55	89.90
05mm/hr Two Layers (Thick layers)	0	0	0	0	0	0.05
05mm/hr Two Layers (Thick layers)	0	0.05	59.30	84.90	99.75	100
05mm/hr Two Layers (Thin layer)	0	0	0	0	7.15	34.40
20mm/hr Two Layers (Thin layer)	0	0.05	71.10	96.95	100	100

Table3: Probability of failure for 1:1.267 slope

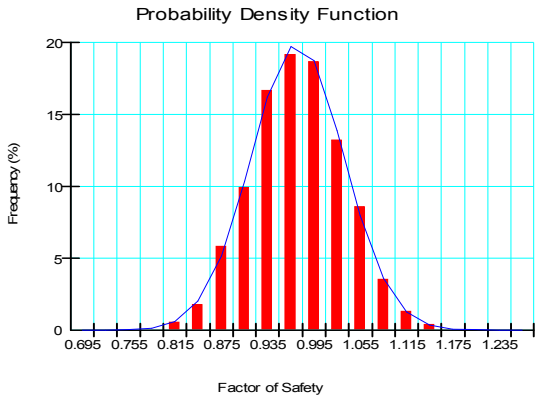

Figure14- Probability density function of two layer system at failure (20mm/hr)

Conclusions

Failures in slopes made of residual soils are often triggered by rainfall. This behavior was clearly illustrated by modeling the infiltration process and analyzing the stability of the slope after incorporating the resulting pore water pressures. The parametric study clearly indicated the effect of the duration and intensity of the rainfall.

It was found that the rainfalls of greater intensity are more detrimental. But rainfall of intensity much greater than the permeability of the soil will contribute to runoff.

It was also illustrated that when a layer of much lower permeability (less weathered rock) underlies the residual soil, the effect of rainfall is more critical than in the case of a uniform residual soil.

The computed probability of failure would provide a more complete picture of the safety of the slope if uncertainties involved in the soil parameters and pore water pressures can be accurately quantified. If the probability of occurrence of a typical rainfall can be estimated with the help of available data, an annual probability of failure could be estimated. This parameter could be used for risk analysis purposes and in the decision making processes to deign appropriate drainage measures to ensure a desired level of safety.

By cutting the slope to a flatter gradient, the safety margins could be increased during the dry season. But prolonged rainfall causes a reduction of the safety margins rapidly.

As such, improvement of surface drainage and minimization of infiltration should be the main activity to ensure the stability of natural and cut slopes in unsaturated residual soils.

References

Fredlund, D.G., Morgenstern,N.R and Widger R.A(1978) “The shear strength of unsaturated soils.” Canadian geotechnical journal, 15, 313-321

Celestino, T. B., and Duncan, J. M. (1981). “Simplified Search for Non-Circular Slip Surfaces, “Proceedings, Tenth International Conference on Soil Mechanics and Foundation Engineering, International Society for Soil Mechanics and Foundation Engineering, Stockholm, A.A. Balkema, Rotterdam, Holland, Vol 3, pp 391-394

GEO-SLOPE International Ltd. (2007). “Stability Modeling with SLOPE/W 2007- An Engineering Methodology” *Calgary, Alberta, Canada*, Second Edition, May 2007.

Krishna. P.A, Rolf .S, Lars. G and Steinar.(2006) “Slope Stability Evaluations by Limit Equilibrium and Finite Element Methods” *Doctoral Thesis at NTNU 2006:66 • ISBN 82-471-7881-8*

US Army Corps of Engineers (2003), “Slope Stability Engineer Manual”, *Department of the Army* ,Washington, USA.

Thavasuthan T[1] and Thilakasiri H. S[2]

Empirical Correlations For Sri Lankan Peaty Soils

ABSTRACT: The composition of natural deposits of peaty soil may vary considerably among different sites, as do their engineering properties. Peat, generally formed in marshy and water logged areas, is usually dark brown to black in colour, has distinctive odour of decaying vegetation, is spongy in consistency without exhibiting distinct plasticity and has amorphous and fibrous texture. As a result, engineering properties of peaty soils are significantly different from most of the inorganic soils. The important engineering properties of the peat are permeability, compression index, coefficient of secondary compression and shear strength. These properties may vary due to chemical and biological conditions. Humification of organic constituents alters the compressibility, shear strength and hydraulic conductivity. There are useful relationships found between index properties and mechanical properties for peaty soils. The preliminary design of structures to be built on peats can profit from these relationships, sometimes even more so than when dealing with clays, due to the difficulty of obtaining high quality peat samples and to the extreme variability of peat deposits. Since the engineering properties of peaty soils are region specific, the empirical correlations for peaty soils found in Southern Transport Development project (STDP) and the updated correlations for Sri Lankan peaty soils are presented in this study.

Introduction

Natural soil deposits composed of plant and organic matter in various stages of decomposition are generally referred to as peat. Peat is mainly found in low lying areas closer to natural water bodies. Peat is usually dark brown to black in colour, has distinctive odours of decaying vegetation, is spongy in consistency without exhibiting distinct plasticity and has amorphous and fibrous texture. It possesses very low strength, high water content and high compressibility characteristics.

Southern Expressway, constructed under the Southern Transport Development Project (STDP), runs through the Western coast to South western coastal area of the island as shown in Figure 1. The area traversed by the proposed Southern Expressway experiences a humid, tropical climate with an average annual rainfall in excess of about 2500 mm. In this region, the flood plains of Wellipenne Ganga and Bentota Ganga are found in the coastal belt. The fluctuation of the water table, due to excessive rainfall during wet season and the drying up during the dry season, provides very favourable conditions for the accumulation of peat deposits in this area, which consist mainly of poorly drained grounds.

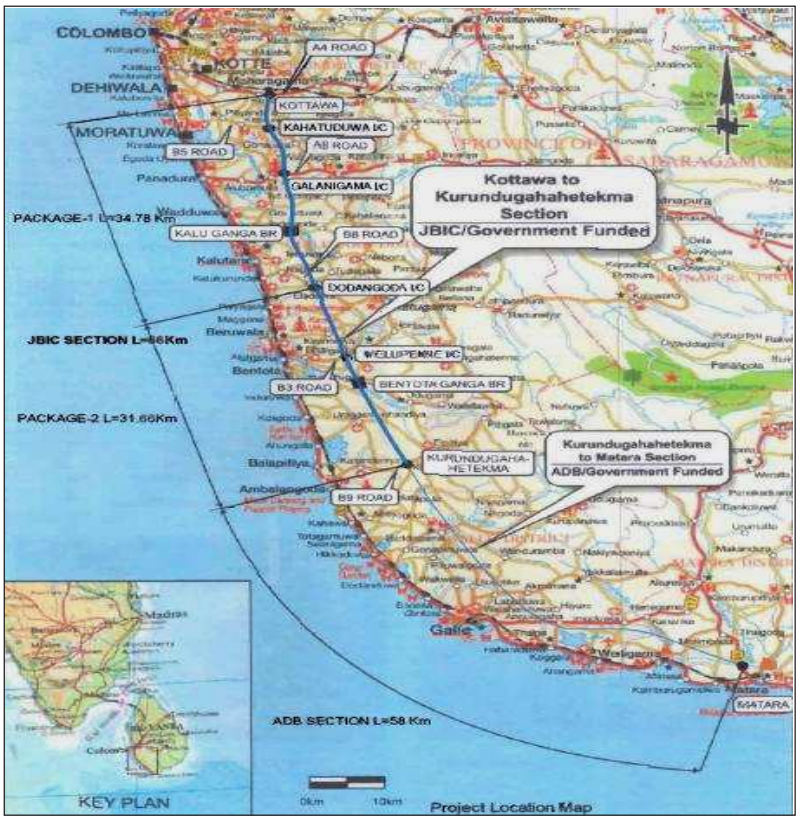

Figure 1 - Alignment of the Southern expressway within STDP.

[1]Graduate, Department of Civil Engineering University of Moratuwa, Sri Lanka
[2]Professor, Department of Civil Engineering University of Moratuwa, Sri Lanka

The engineering properties of the peat are permeability, compression index, coefficient of secondary compression and shear strength. These properties may vary due to the chemical and biological conditions of the surrounding environment. Humification of organic constituents alters the compressibility, shear strength and hydraulic conductivity.

For engineering purposes, peat is categorized into three main groups: "amorphous-granular peat" (i.e. well decayed peat), "Fine fibrous peat" and "Coarse fibrous peat" (Radforth, 1969). The amorphous-granular peat has high colloidal mineral element and tends to hold their water locked in an adsorbed state surrounding the grain structure like clay. The two fibrous peat types," Fine fibrous" and "Coarse fibrous", are woodier and hold most of their water within the peat mass as free water. These basic groups generally reflect how the peat deposits grew and govern the main engineering properties.

Rapidly increasing population has demanded rapid infrastructure development projects linking major city centers in the country. Most of these infrastructure projects run through marshy lands consisting of relatively thick peaty deposits. Due to the high compressibility characteristics and the time dependent nature of the associated settlement, the compressibility and permeability properties of peaty soils are very essential for design purposes. However, due to the very low shear strength it is extremely difficult to recover undisturbed peaty samples for laboratory testing to obtain the required engineering properties. Therefore, in this study it is intended to obtain empirical correlations to determine compressibility and permeability properties of peaty soils from simple index properties such as water content, void ratio, and organic content.

Methodology

Engineering properties of peaty soils are significantly different from those of most inorganic soils. Most peat deposits are highly variable (Hanrahan 1954; Lnadva and La Rochelle 1983). This characteristic, related mainly to variable degree of decomposition within peaty soil deposit, has been a serious impediment to accurate interpretation of the behaviour of peaty soil deposits from laboratory measurements and field observations [e.g., Magnan (1994)]. The other obstacle to laboratory testing of peaty soils and interpretation of laboratory measurements is the potential for biodegradation of peat in laboratory environment (Mesri et al.1997).

This paper presents empirical relationships of the engineering properties of peaty soils in the Southern Expressway project including permeability, and compressibility using data obtained from laboratory tests from undisturbed samples. Undisturbed samples of 70 mm diameter were obtained from different depths in various locations throughout the highway alignment for this purpose. From the one dimensional consolidation test, initial void ratio (e_0), primary compression index (C_c), recompression index (C_r) and initial water content (w_0) were determined. Long term consolidation tests were done to determine the coefficient of secondary consolidation. Organic contents of these samples were also determined. The summary of engineering properties obtained from laboratory tests are shown in Table 1.

Item	Properties	Peaty Soils
1	Natural Moistue Content (%)	141.7 - 523.7
2	Bulk Density (g/cm$^{2)}$	0.94 - 1.02
3	Dry Density (g/cm^2)	0.16 - 0.22
4	Organic matte content (%)	17.0 - 92.0
5	Initial void ratio e_0	1.56 - 9.35
6	C_c	1.06 - 4.53
7	C_s	0.021 - 0.46
8	C_α	0.81 - 0.145

Table 1 – The variation of the properties of peaty soils from Southern Expressway project within STDP.

The relationship between compression index C_c and initial water content (w_0), compression index C_c and initial void ratio (e_0), coefficient of secondary consolidation C_a and compression index C_c, recompression index C_r and compression index Cc, compression index C_c and organic content, coefficient of secondary consolidation C_α and organic content, $C_k = D_e / D \log k_v$ and the initial void ratio e_0 were studied in this research. Moreover, the developed correlations are compared with the other established correlations by Karunawardane (2000) and updated correlations are also proposed by combining with the results from already published previous research.

Data Analysis

Compressibility of Peaty Soils

Primary and secondary compressibility properties of peaty soils are extremely useful to estimate the primary and secondary consolidation settlements of peaty soils. Primary compression can be observed during the increase in the effective vertical stress and the secondary compression can observed after primary compression under a constant effective vertical stress. The compressibility of peaty soils depends on in-situ void ratio and arrangement of soil particles.

Relationship between compression index (C_c) and the natural water content (w_0)

The relationship between compression index (C_c) and the natural water content (w_0) of STDP peaty soils is shown in Figure 2a. There is some scatter in the data normally associated with peat, the majority of the results confirm the $C_c = 0.0072\ w_0$ relationship for the peaty soils found in STDP.

Same relationship for peaty soils in Sri Lanka was proposed by Karunawardena (2000) is $C_c = 0.007\ w_0$. The updated relationship using STDP peaty soils and Karunawardana (2000) is shown in Figure 2b. The same relationship of C_c versus (w_0) for UK fen peat and the UK bog peat are Cc = $0.0065\ w_0$ and $Cc = 0.008\ w_0$ respectively (Hobbs 1986).

It is clear from Figure 2a that all the soil samples considered from the STDP are having natural water contents more than 100%. As the natural water content is directly proportional to the organic content, majority of the peaty samples from STDP are having a high organic content compared to the soil samples considered in Karunawardane (2000). This observation is confirmed by the organic content of some of the samples later presented in Figure

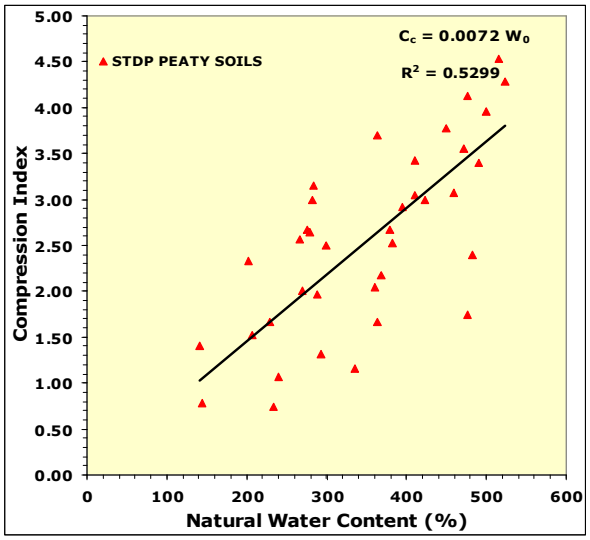

Figure 2a - C_c vs w_0 (%) relationship for STDP peaty soils.

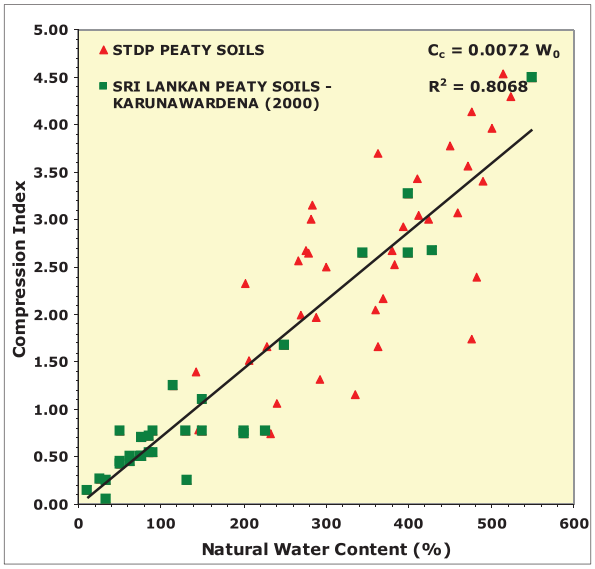

Figure 2b - C_c vs w_0 (%) updated relationship for Sri Lankan peaty soils.

5a and 5b. The combined data shown in Figure 2a covers a wider range of water content and hence, the relationships developed with combined data are more representative of organic soils in general.

Relationship between compression index C_c and initial void ratio e_0

The relationship between compression index C_c and initial void ratio e_0 for STDP soils is shown in figure 3a. Figure 3a shows that the majority of the results falls into the Cc= 0.468 e_0 relationship. The observed and the reported relationship for C_c

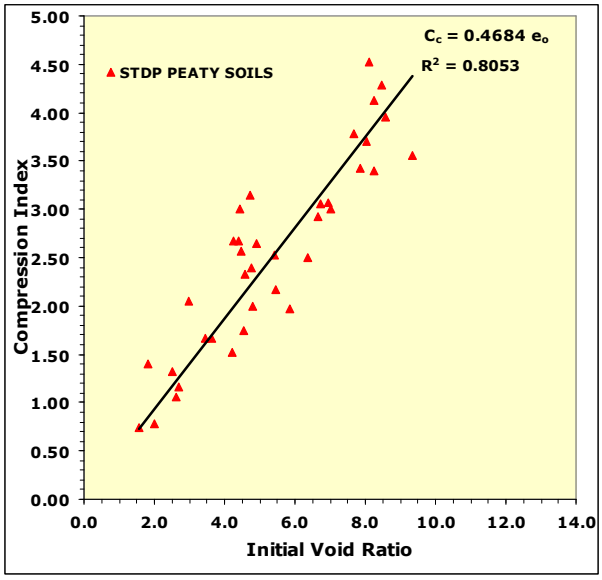

Figure 3a C_c vs. e_0 relationship for STDP peaty soils.

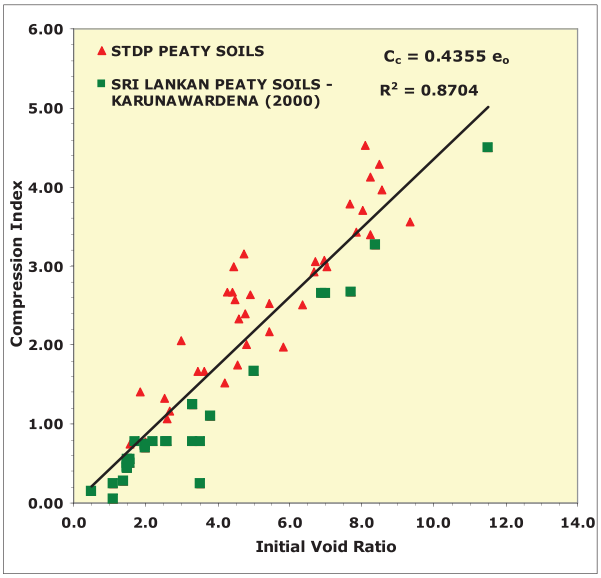

Figure 3b - C_c vs. e_0 updated relationship for Sri Lankan peaty soils.

and e_0 for peat found in the UK is $C_c = 0.45e_0$ (Hobbs 1986) and the same for Sri Lankan peaty soils reported by Karunawardena (2000) is $C_c = 0.367e_0$.

The updated relationship for STDP peaty soils is shown in Figure 3b. The updated relationship of C_c = 0.4355 e_0 is close to the same observed from UK peaty soils.

Secondary Compression:

Secondary compression behaviour of soft soil is completely explained and predicted by the C_a / C_c law of compressibility (Mesri and Godlewski 1977,1979; Mesri and castro 1987; Mesri 1987 ; Mesri et al. 1994a, 1997). Secondary compression is often more significant in peat deposits than in other geotechnical materials (Mesri 1997). Peat deposits have very high natural water contents and void ratios.

The values of C_α/C_c for all geotechnical materials are in the range of 0.01 to 0.07. An important aspect of C_α/C_c law of compressibility is the very narrow range of values of C_α/C_c for all geotechnical materials considered together. The magnitude of the C_α/C_c appears to depend on compressibility and deformability of the soil particles. Peaty soils display highest values for C_α/C_c due to the open structure of the peat lattice and its structural form consisting of an intricate system of cells and baffle walls.

Due to high in situ void ratios, peat deposits display high values of compression index C_c. In addition, as C_α is directly related to C_c, peat deposits display high C_α. The relationship between C_α

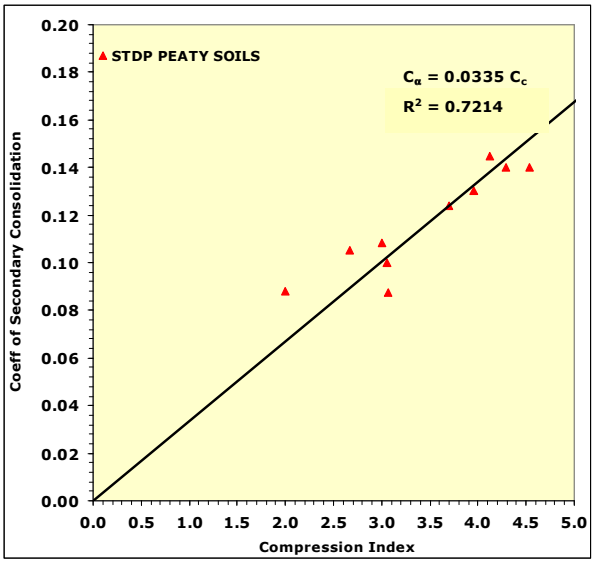

Figure 4a C_a vs. C_C relationship for STDP peaty soils.

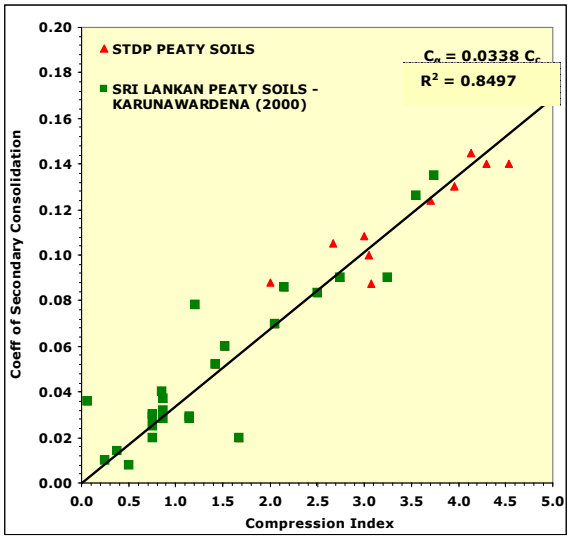

Figure 4b C_α vs C_c updated relationship for Sri Lankan peaty soils

and C_c for STDP peaty soils is $C_\alpha = 0.0335\ C_c$. Figure 4a shows relationship between C_α and C_c for STDP peaty soils.
The relationship predicted by Karunawardena (2000) is $C_\alpha = 0.0341\ C_c$. The updated relationship by using STDP soils for Sri Lankan peaty soils is $C_\alpha = 0.0338\ C_c$ as shown figure 4b.

Relationship between compression indexes C_c, C_α and the organic content (OC)

As shown in Figure 5a, the compression index (C_c) of the peat found in STDP increases with an increase in the organic content (OC). Similar to the relationship between the compression index and the organic content, the coefficient of secondary consolidation

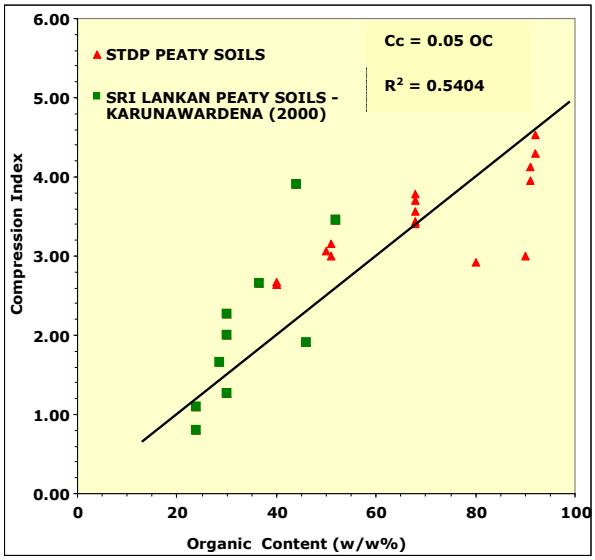

Figure 5a C_c vs. OC relationship for Sri Lankan peaty soils.

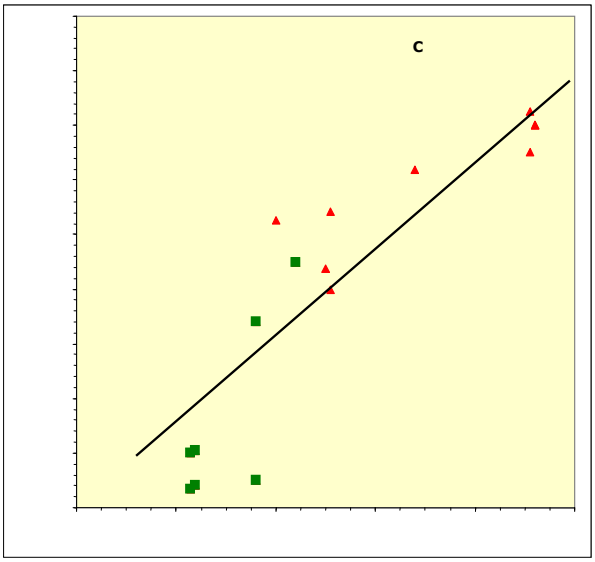

Figure 5b C_α vs. OC relationship for Sri Lankan peaty soils.

(C_α) shows an increase in creep characteristics with the increase in the organic content, as shown in Figure 5a. The observed results by Karunawardena (2000) presented in Figure 4b and Figure 5b. The majority of the results for Sri Lankan peaty soils falls into the $C_c = 0.05$ OC relationship with R^2 of 0.5404 and $C_\alpha = 0.0016$ OC relationship with R^2 of 0.7963.

Relationship between recompression index C_r and C_c

The relationship between the recompression index (C_r) and the compression index (C_c) from laboratory tests for STDP peaty

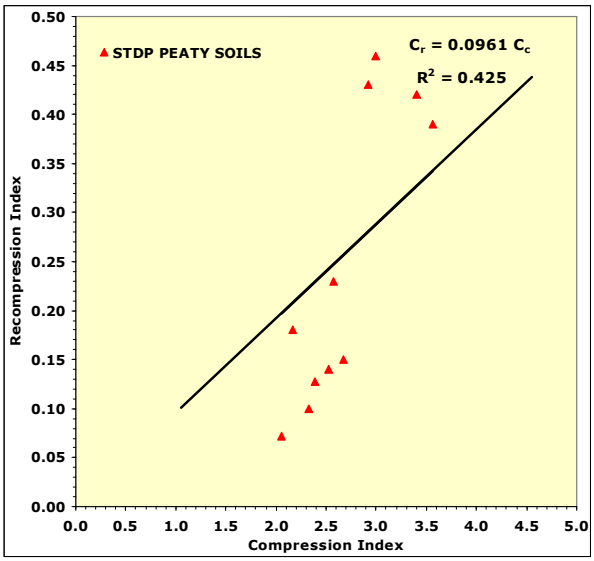

Figure 6a C_r vs. C_C relationship for STDP peaty soils.

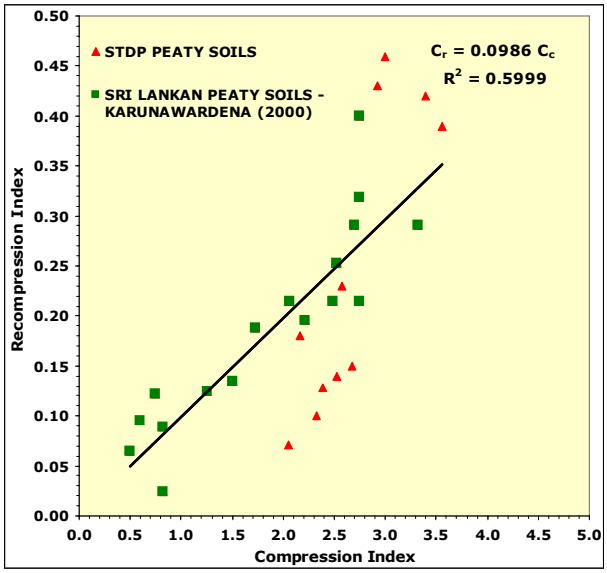

Figure 6b C_r vs. C_c updated relationship for Sri Lankan peaty soils.

soils is given in Figure 6a. It shows that the two parameters are related and that the average, C_r is about 10% of C_c. The observed relationship for STDP peaty soils shows $C_r = 0.0961C_c$ which is closer to the relationship of $C_r = 0.1058C_c$ established by Karunawardena (2000). The updated relationship shows C_r = 0.0986 C_c with R^2 of 0.5999. The updated relationship is shown in Figure 6b

Permeability of Peaty Soils

The permeability of all soils is dependent on the void ratio, size of flow channels perpendicular to the direction of flow, and shape of flow channels parallel to the direction of flow. The relationship between void ratio (e) and log effective stress ($\log(s')$) and relationship between void ratio (e) and log permeability ($\log(k_v)$) are useful in interpretation of time period for the primary consolidation.

These relationships show reduction in permeability (k_v) with the increase in effective vertical stress (s') and decrease in void ratio (e), where kv is the dependent variable and e is the independent variable. Therefore, the slope of e versus log k_v that is, $C_k = De / D \log k_{v,}$ is commonly used to characterise decrease in permeability with decrease in void ratio. When C_k is very large, then for given

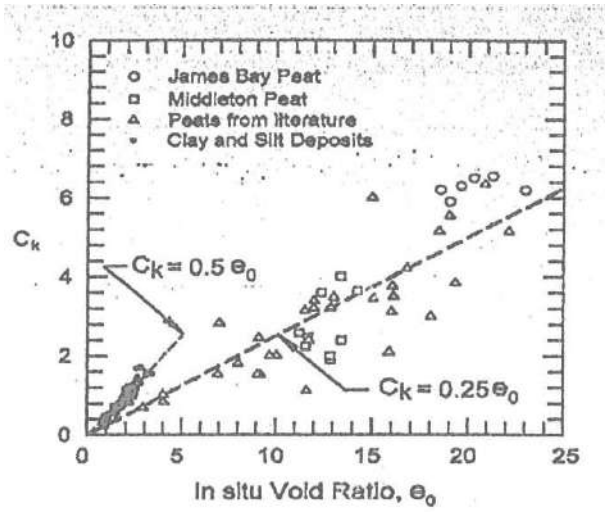

Figure 8 Relationship between C_k and in situ void ratio (e_0)

decrease in void ratio the decrease in permeability is very small and vice versa.

Peaty soil particles are large compared to the size of other soil particles and peaty soil possesses an open porous structure. Therefore, peaty soils exist at very high void ratios and display high initial permeability. As mentioned earlier due to large compressibility, their permeability decreases dramatically as they are compressed under external loads such as embankment loads. The empirical relationship for peaty soils can be given as:

$$C_k / e_0 = 0.25 \qquad (1)$$

Same relationship for soft clays(Tavenas et al 1983; Mesri et al. 1994b) can be given as:

$$C_k / e_0 = 0.50 \qquad (2)$$

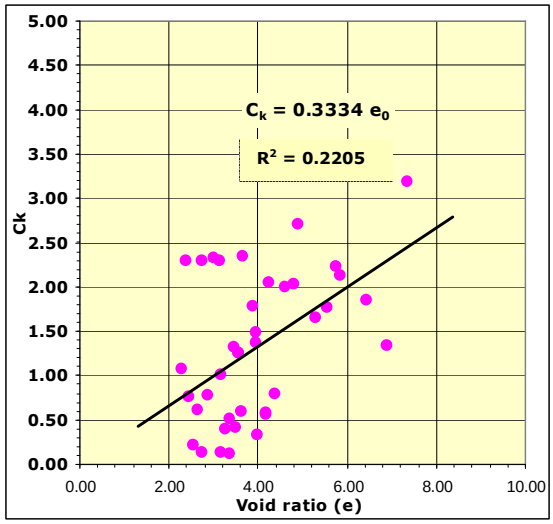

Figure 9a C_K vs. e_0 relationship for STDP peaty soils.

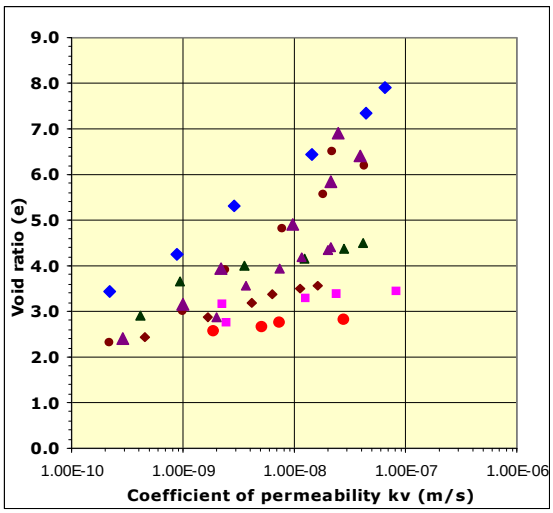

Figure 9b C_k vs log k_v relationship for STDP peaty soils

Figure 8 shows the relationship between C_k and in situ void ratio (e_0) for soft clays and peaty soils.

The relationships between C_k and initial void ratio (e_0), initial void ratio (e_0) and log k_v are shown in figures 9a and 9b respectively. The results yields the relationship of $C_k = 0.334\ e_0$ with R^2 of 0.2205.

Interpretation of results

The empirical correlations between properties of peaty soils obtained from STDP were established and the relationships between the soil parameter, for STDP peaty soils and correlations proposed by Karunawardena (2000) were compared. The updated correlations for Sri Lankan peaty soils by combining data from STDP and other previous research are presented below.

a. The updated relationship of $C_c = 0.0072\ w_0$ between compression index C_c and the natural water content (w_0) using STDP peaty soils, shows good agreement with existing relationship of $C_c = 0.007\ w_0$ (Karunawardena 2000).

b. Slightly improved relationship of $C_c = 0.4355\ e_0$ between compression index C_c and initial void ratio (e_0) using STDP peaty soils.

c. The new relationship for Sri Lankan peaty soils was obtained between C_c and organic content (OC) and C_α and organic content (OC). The relationships shows $C_c = 0.05\ OC$ relationship and $C_\alpha = 0.0016\ OC$.

d. The updated relationship of $C_\alpha = 0.0338\ C_c$ between secondary compression index C_α and compression index using STDP peaty soils.

e. Similarly recompression index also showed slightly improved correlation of $C_r = 0.0986\ C_c$.

f. Finally new relationship of $C_k = 0.334\ e_0$ was established between C_k and initial void ratio (e_0).

The summary of updated correlation for Sri Lankan Peaty Soils is shown in Table 2.

Table 2 – Summary of the correlations.

Relationship	STDP soils	Karunawardena (2000)	Updated
C_c vs. W_o	$Cc = 0.0072\ W_o$	$C_c = 0.0070\ W_o$	$C_c = 0.0072\ W_o$
C_c vs. e_o	$Cc = 0.4684\ e_o$	$C_c = 0.3670\ e_o$	$C_c = 0.4355\ e_o$
C_c vs.OC	$Cc = 0.0500$ OC	-	-
C_α vs.OC	$C_\alpha = 0.0016$ OC	-	-
C_α vs.C_c	$C_\alpha = 0.0335\ C_c$	$C_\alpha = 0.0341\ C_c$	$C_\alpha = 0.0338\ C_c$
C_r vs.C_c	$C_r = 0.0961\ C_c$	$C_r = 0.1058\ C_c$	$C_r = 0.0986\ C_c$
C_α vs.e_o	$C_\alpha = 0.334\ e_o$	-	-

Conclusions

In the present study, empirical correlations for the STDP peaty soils are developed and combined with the already proposed correlations by Karunawardane (2000) to update the same. The combined data from the Karunawardane (2000) and the present study represent organic soils with a wider range of organic contents and hence, the updated correlations represent the organic soils better than the two studies considered individually. This point is proved by the fact that the updated (or combined) correlations compare well with the similar correlations proposed in other countries.

A summary of the developed correlations are presented below.

1. The updated relationship between C_c and w_0 for Sri Lankan peaty soils is $C_c = 0.0072\ w_0$. This lies between the relationships for UK fen peat, $C_c = 0.0065\ w_0$, and for UK bog peat, $C_c = 0.008\ w_0$, (Hobbs, 1986).

2. Improved relationship between C_c and e_0 for Sri Lankan peaty soils is $C_c = 0.4355\ e_0$. This value shows closer agreement with peaty soils found in UK (Hobbs 1986).

3. The relationship between C_c and organic content, C_α and organic content for Sri Lankan peaty soils are $C_c = 0.05\ OC$ and $C_\alpha = 0.0016\ OC$.

4. The updated relationship between C_a and C_c for Sri Lankan peaty soils is $C_\alpha = 0.0338\ C_c$. The same relationship for Middleton peat, UK(Mesri et al.1997) is $C_\alpha = 0.052\ C_c$.

5. The recompression index also showed slightly improved correlation of $C_r = 0.0986\ C_c$ with existing co correlation.

6. Relationship between $C_k = De/D \log k_v$ and e_0 is $C_k = 0.334\ e_0$.

References:

Hanrahan, E. T. (1954). "*An Investigation of Some Physical Properties of Peat.*" *Geotechnique*, **4**(3), pp.103-123.

Magnan , J.P.(1994). "Construction on peat: State of the art in France." Proc., Int. Workshop on Advances in Understanding and Modelling the mechanical Behaviour of Peat, E. den Haan, R. Tremaat, and T.B. Edil, eds., Balkema, Delft, The Netherlands, 369-379

Karunawardena, A. (2007). *Consolidation Analysis of Sri Lankan Peaty Clay using Elasto-viscoplastic Theory*. Doctoral Thesis, Kyoto University, Japan.

Karunawardena, W.A. (2000) "A Study of Consolidation Characteristics of Colombo Peat", *Proceedings of 1st International Young Geotechnical Engineering Conference*, Southampton, United Kingdom.

Lnadva, A.O., and La Rochelle P (1983). "Compressibility and shear characteristics of Radforth peats." Testing of peat and organic soils, STP 820, ASTM ,WEST Conshohocken, pa., 157-197.

Magnan , J.P.(1994). "Construction on peat: State of the art in France." *Proc., Int. Workshop on Advances in Understanding and Modelling the mechanical Behaviour of Peat*, E. den Haan, R. Tremaat, and T.B. Edil, eds., Balkema, Delft, The Netherlands, 369-379

Mesri, G.(1987). "Fourth law of soil mechanics: A law of compressibility" *Proc. Int. Symp. on Geotechnical Engineering of soft soils*, Vol.2, M.J Mendoza and L.Montanez, eds., Sociedad Mexicana de Mecanica de Suelos, Coyocan, Mexico,179-187.

Mesri,G. & Ajlouni,M. 2007. "Engineering properties of fibrous peats", *J. of Geotechnical Engineering, ASCE*, 133(7): 1090–0241.

Mesri, G., Castro, A. (1987). "The C_α / C_C Concept and Ko during Secondary Compression.", *Journal of Geotechnical Engineering*, ASCE, **112**(3), pp.230-247.

Mesri, Feng , T.W., Ali, S., and Hayat, T.M.(1994a)."Permeability characteristics of soft clays." *Proc., 13th Int. Conf on Soil Mechanics and Foundation Engineering*, Vol..2, balkema, Rotterdam, The Netherlands, 187-192

Mesri, G., Godlewski, P. (1977). "Time and Stress – Compressibility Interrelationship." *Journal of Geotechnical Engineering Division, Vol. **103***, No. GT5, pp.417-430

Mesri, G. & Godlewski, P.M. (1979) Closure: Time- and stress-compressibility interrelationship, *Journal of Soil Mechanics and Foundation Division*, ASCE,

105(1), 106

Mesri, G., Stark, T.D., Ajlouni, M.A. & Chen, C.S. (1997), "Secondary compression of peat with or without surcharging", *Journal of Geotechnical Engineering*, ASCE,

123(5), 411- 421

Radforth, N.W. (1969). *Muskeg Engineering Handbook*. Eds Macfarland, I.C., University of Toronto Press.

Tavenas, F., Jean, P., Leblond, P., and Leroueil, S.(1983). "Permeability of natural soft clays. II Permeability characteristics." Can. Geotech. J., 20(4), 645-660

Information for Authors

The Journal provides an opportunity to present research findings, case studies and field experiences in Geotechnical and related fields. It would also publish invited papers and memorial lectures. Each published paper and technical note will be peer-reviewed. Papers and technical notes are open to brief written comments in the Discussion Section of the Journal, which also includes authors' written responses.

The Editorial Board of the SLGS may consider a paper submitted to the Journal as a technical note if it gives a reasonably brief description of on going studies with or without providing interim, tentative data, conclusions; and it reports phenomena observed in the course of research requiring further study; it provides mathematical procedures for facilitating reduction and analysis of data; or it reports promising new materials prior to undertaking extensive research to determine their properties.

The decision as to whether a manuscript is published as a paper or a technical note resides with the editorial board; on recommendations made by the reviewers. The guidelines below describe our manuscript selection. Peer review, revision, and publication processes.

Submission:

The name, mailing address, position, affiliation, and telephone / fax of each author must be supplied in a cover letter, addressed to secretary, Sri Lankan Geotechnical society, c/o National Building Research Organisation, 99/1 Jawatte Road, Colombo 5, Sri Lanka. Also, a statement to be included that the paper has not been published and it is not under consideration for publication elsewhere. All permissions for previously published material used in the paper must be submitted in writing at this time. The submitting author must also affirm that all those listed as co-authors has agreed a) to be listed and b) to submit the manuscript to SLGS for publication.

Three copies of the manuscript with clear copies of each figure are required.

Manuscript Instructions

The hard-copy text can be produced on any letter-quality printer. Authors require the use of SI units in all publications (including figures and tables). If fps units must be used to describe materials and present test results, SI equivalents must follow in parenthesis.

All tables are to be placed together at the end of the manuscript preceding the illustrations. Tables are to be numbered in Arabic and are cited in numerical order in the text. All tables and figures should be prepared in single portrait page format.

Each figure is to be simple and uncluttered. The size of type in illustrations must be large enough to be legible. All lettering, lines, symbols, and other marks must be drawn in black India ink on white paper. Computer graphics must be produced by a laser printer. Photographs must be high-contrast black and white. Scale markers must be shown on all photographs and all figures that are representations of equipment or specimens.

References shall be cited in the text by author's last name and date of publication. References shall be listed together at the end of the text in alphabetical order by author's last name. They must contain enough information to allow a reader to consult the cited material with reasonable effort.

Copyright

The SLGS requires that the submitting author shall return the revised paper assigning copyright to SLGS.

Manuscript Review

The Editorial Board process for peer review, only if the manuscript fits the scope of the journal, will be of interest to the readership, and is well written.

Two or more reviewers, selected by the Editorial Board review each paper for technical content, logical conclusions sound data, reproducibility of results, and clarity of presentation; two or more reviewers provide reviews of each technical note. Their comments are compiled and evaluated. The reviewers' anonymous comments and any other comments from the editor are then returned to the author for revision.

The author must submit three copies of the revised manuscript with an annotated (highlighted) version of the paper indicating clearly where each revision has been made and identifying the reviewers comment to which the revision is responding. Changes in the text including all mandatory reviewers' comments must be addressed explicitly, as well as any explanation why a change was not made.

The authors are requested to submit a computer disk containing the revised manuscript, on Microsoft Word.

The Editorial Board may a) accept the revised manuscript for publication, b) require further revision or explanation,c) decide when reviewers disagree or d) reject the revised manuscript. A revised manuscript may be sent for re-evaluation to a reviewer who has found major flaws in the original manuscript.

Each accepted paper is edited for style, organisation, and proper English usage.

Geotechnical Journal, SLGS, Volume 5, Number 1, DECEMBER 2011

Printed by: R M R Adds, No. 215 A, - Kadawatha Road, Nedimala, Dehiwala - 077 3413060